

Combined NMR Analysis of Huge Residual Dipolar Couplings and Pseudocontact Shifts in Terbium(III)-Phthalocyaninato Single Molecule Magnets

Marko Damjanovic,[†] Keiichi Katoh,^{‡,§} Masahiro Yamashita,^{‡,§} and Markus Enders*[†]

Institute of Inorganic Chemistry, University of Heidelberg, Im Neuenheimer Feld 270, D-69120 Heidelberg, Germany; Department of Chemistry, Graduate School of Science, Tohoku University, 6-3 Aramaki-Aza-Aoba, Sendai 980-8578, Japan; JST, CREST, 4-1-8 Honcho, Kawaguchi, Saitama 332-0012, Japan

* To whom correspondence should be addressed. Tel: +49-6221-546247, Fax: +49-6221-541616247, E-mail: markus.enders@uni-hd.de

[†] University of Heidelberg [‡] Tohoku University [§] CREST (JST)

Supporting Information

Table of Contents:

I. ¹ H and ¹³ C NMR spectra of complex 1 in CD ₂ Cl ₂ (Fig. S1-S13).....	S2
II. The model for fitting the ¹³ C NMR pseudocontact shifts (Fig. S14-S18, Table S1-S15).....	S10
III. ¹ H and ¹³ C NMR spectra of complex 1 in toluene-d ⁸ (Fig. S19-S21, Table S16-S17).....	S22
IV. Isointensity plots and estimated pseudocontact shifts (Eq. S1-S6, Fig. S22-S23, Table S18-S19).....	S25
V. ¹ H NMR pcs according to the model established for fitting the ¹³ C NMR data (Table S20-S22).....	S30
VI. Measured total couplings (Table S23-S26).....	S33
VII. Dynamic frequency shifts (Eq. S7-S11, Fig. S24, Table S27-S29).....	S35
VIII. Residual dipolar couplings and the order parameter (Fig. S25-S26, Table S30-S36).....	S39
IX. Additional information (Eq. S12-S14, Fig. S27-S29, Table S37).....	S43
X. Experimental section (Table S38).....	S46
XI. X-ray structure of complex 1 (Fig. S30-S32).....	S49
XII. Literature.....	S51

I. ^1H and ^{13}C NMR spectra of complex **1** in CD_2Cl_2 (Fig. S1-S13)

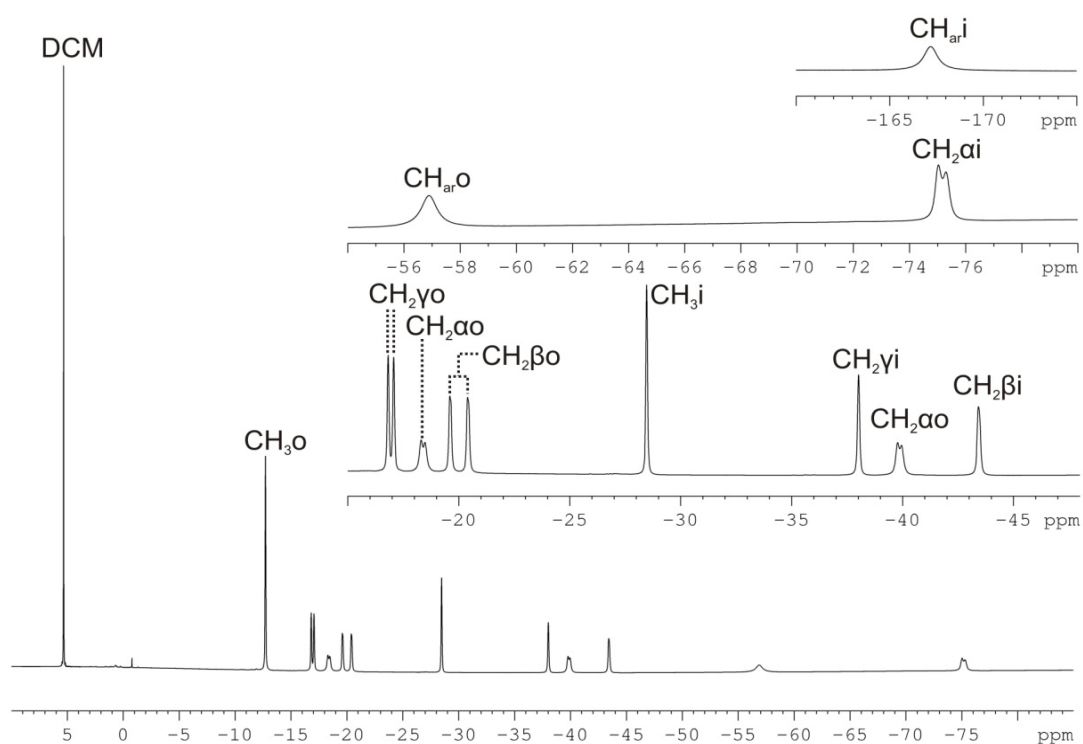


Figure S1. ^1H NMR spectrum of **1** dissolved in CD_2Cl_2 , with selected enlarged segments and annotations of assignments. Spectrum was recorded at 14.09 T, at a temperature of 295.0 K.

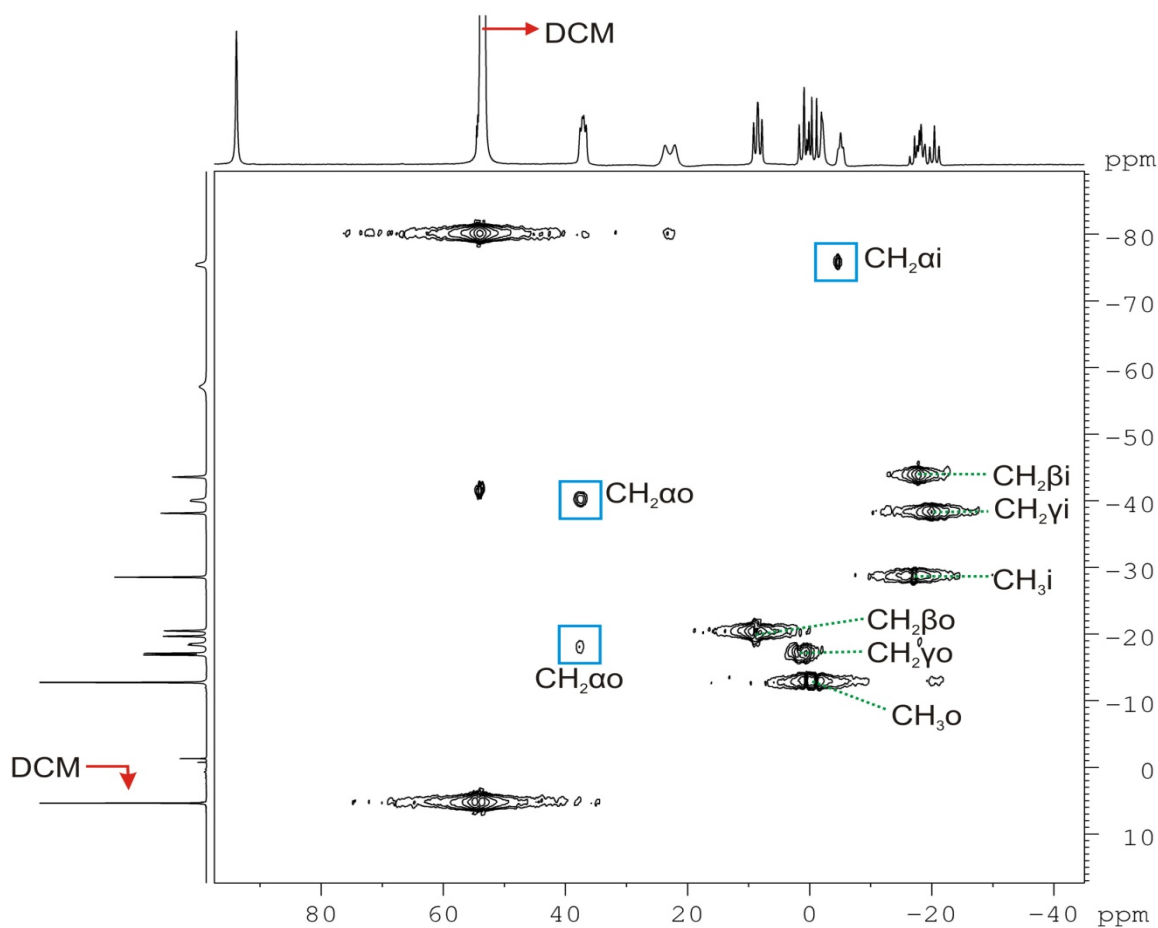


Figure S2. ^1H , ^{13}C NMR correlation spectrum (HETCOR, ^{13}C in F2, horizontal) of compound **1** dissolved in CD_2Cl_2 , recorded at 14.09 Tesla, at a temperature of 295.0 K. The crosspeaks of all the aliphatic groups are present. The assignments of aromatic resonances, that did not show crosspeaks in this experiment due to their fast relaxation, were made based on the values of the observed chemical shifts.

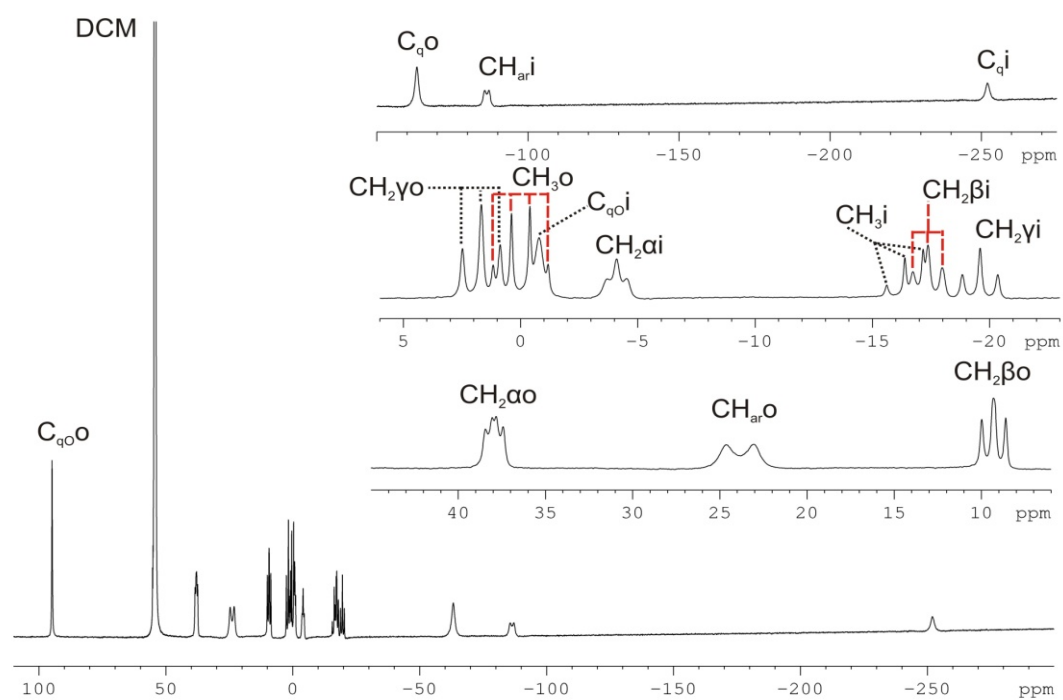


Figure S3. ^{13}C NMR spectrum of **1** dissolved in CD_2Cl_2 , with assignments. Spectrum was recorded at 14.09 T, at a temperature of 295.0 K.

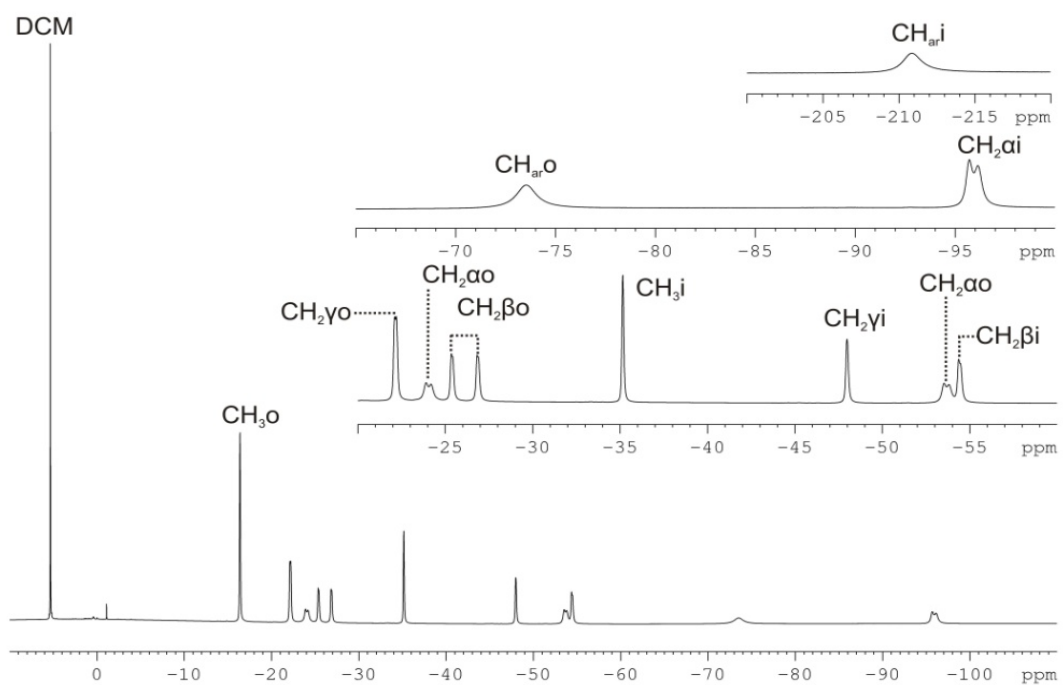


Figure S4. ^1H NMR spectrum of **1** dissolved in CD_2Cl_2 , with assignments. Spectrum was recorded at 14.09 T, at a temperature of 265.0 K.

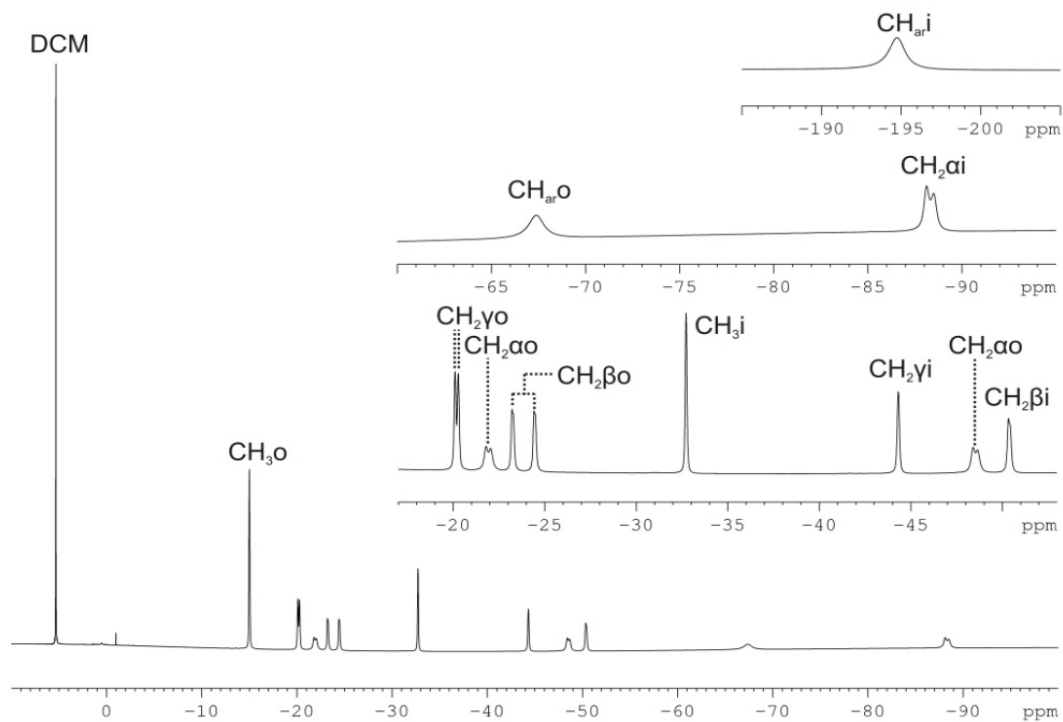


Figure S5. ^1H NMR spectrum of **1** dissolved in CD_2Cl_2 , with assignments. Spectrum was recorded at 14.09 T, at a temperature of 275.0 K.

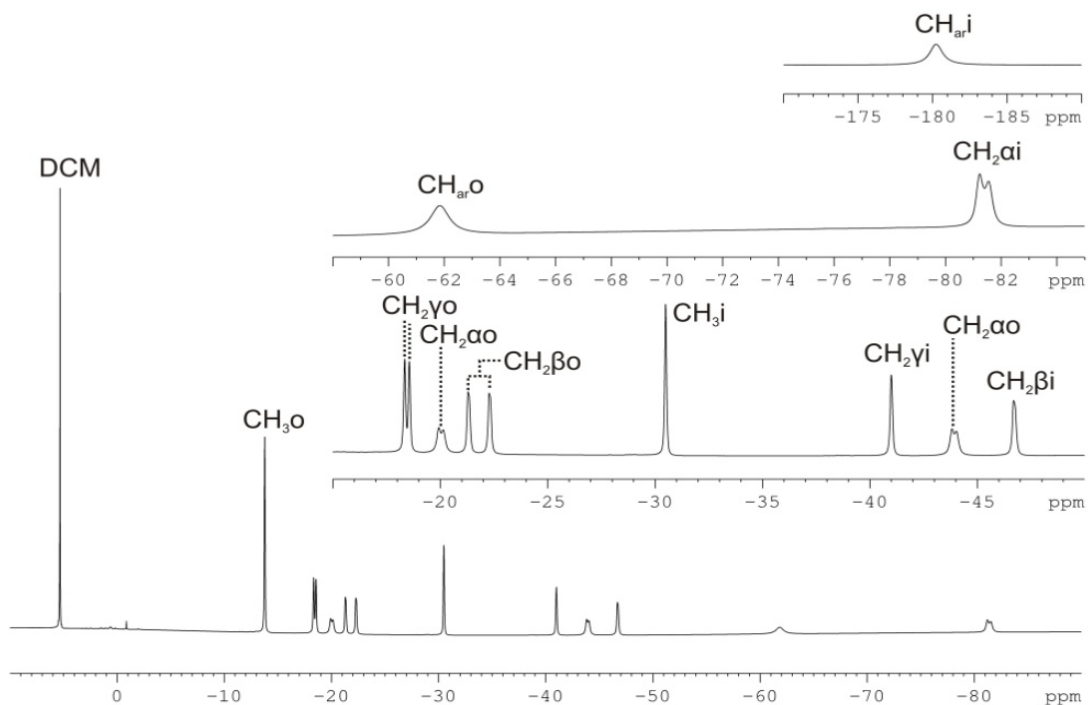


Figure S6. ^1H NMR spectrum of **1** dissolved in CD_2Cl_2 , with assignments. Spectrum was recorded at 14.09 T, at a temperature of 285.0 K.

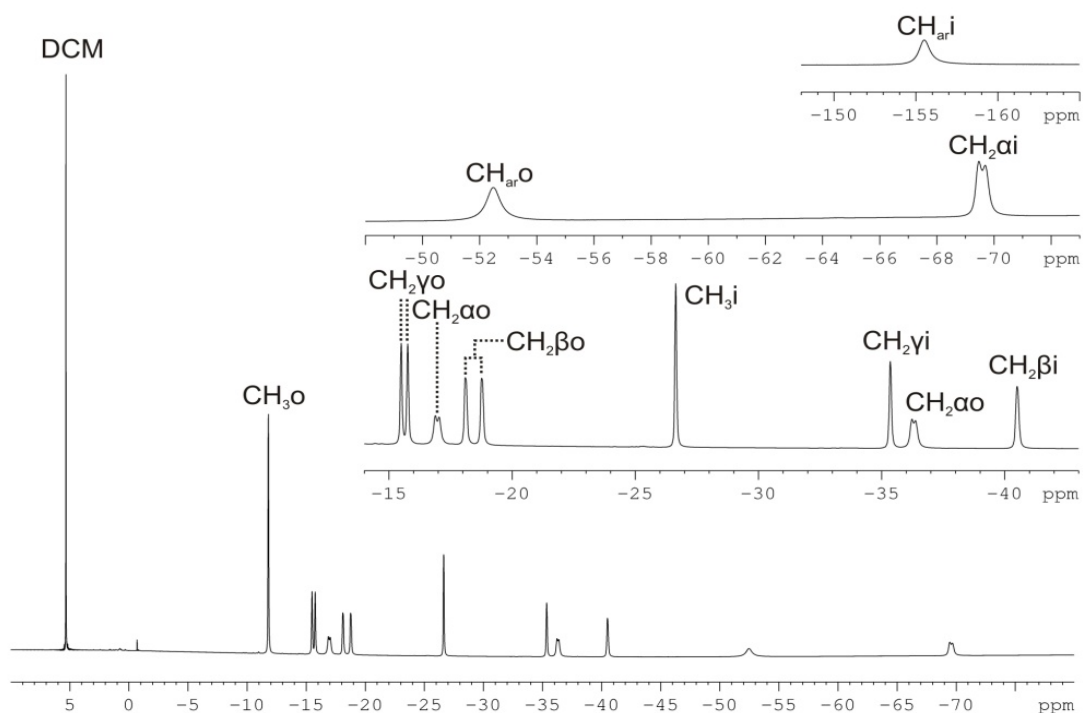


Figure S7. ^1H NMR spectrum of **1** dissolved in CD_2Cl_2 , with assignments. Spectrum was recorded at 14.09 T, at a temperature of 305.0 K.

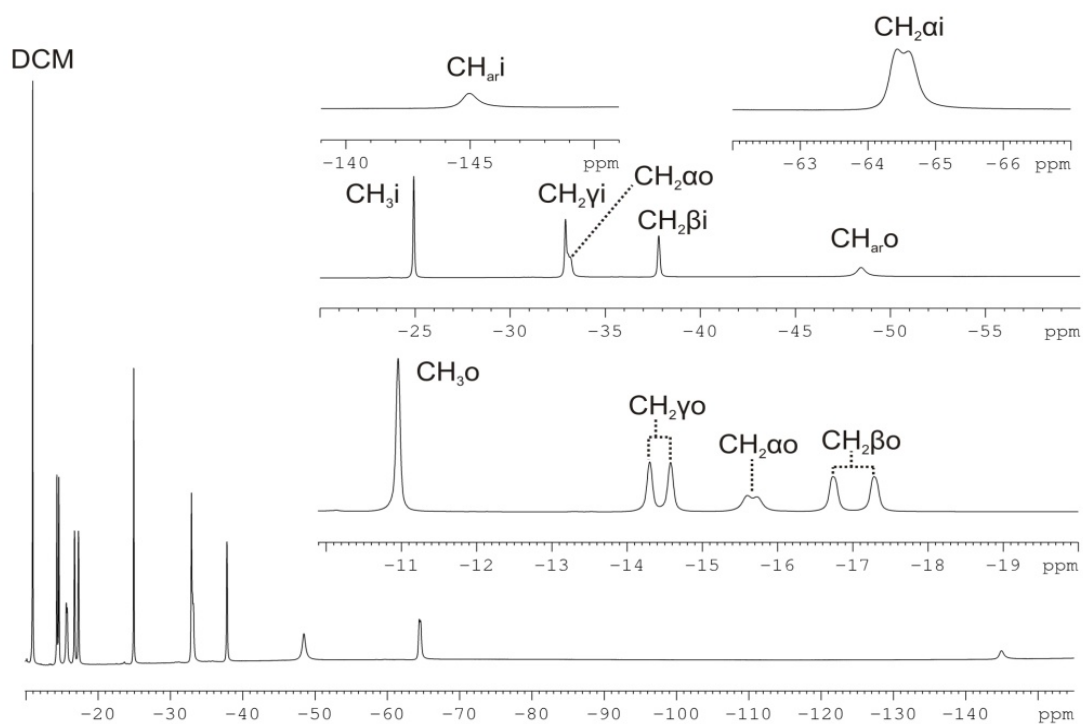


Figure S8. ^1H NMR spectrum of **1** recorded in CD_2Cl_2 , with assignments. Spectrum was recorded at 14.09 T, at a temperature of 315.0 K.

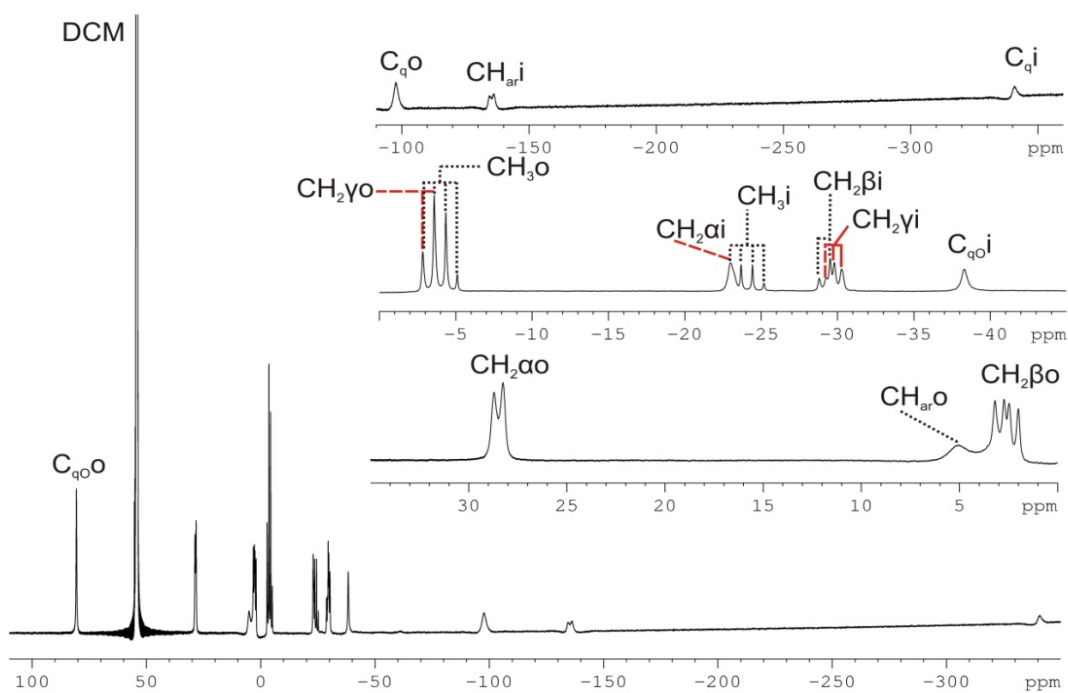


Figure S9. ^{13}C NMR spectrum of **1** dissolved in CD_2Cl_2 , with assignments. Spectrum was recorded at 14.09 T, at a temperature of 265.0 K.

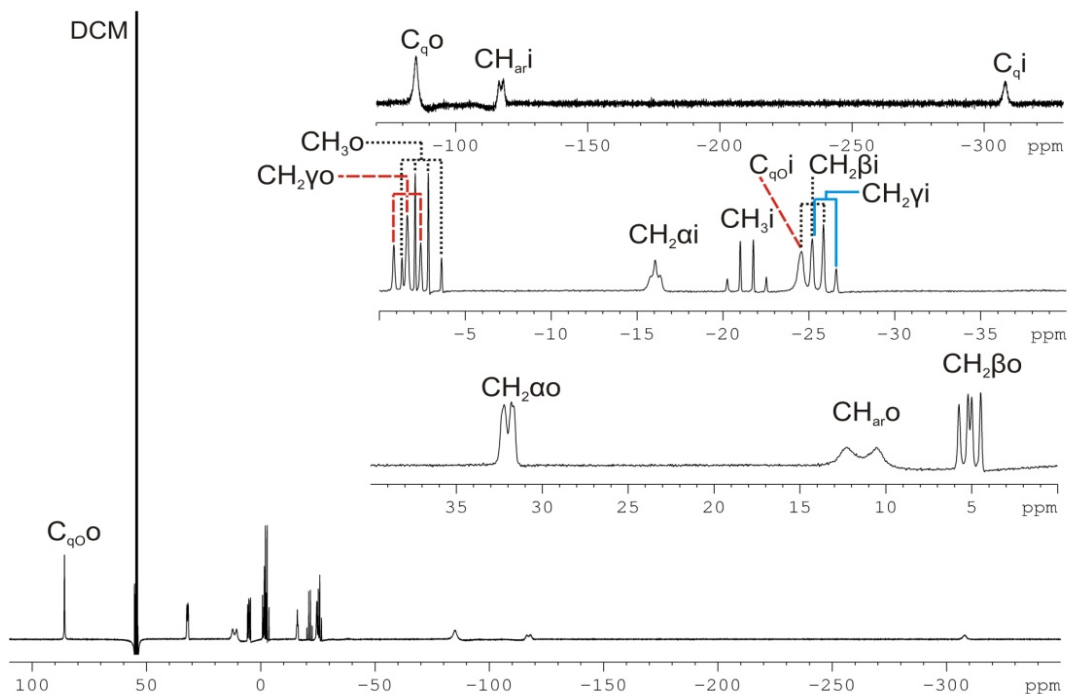


Figure S10. ^{13}C NMR spectrum of **1** dissolved in CD_2Cl_2 , with assignments. Spectrum was recorded at 14.09 T, at a temperature of 275.0 K.

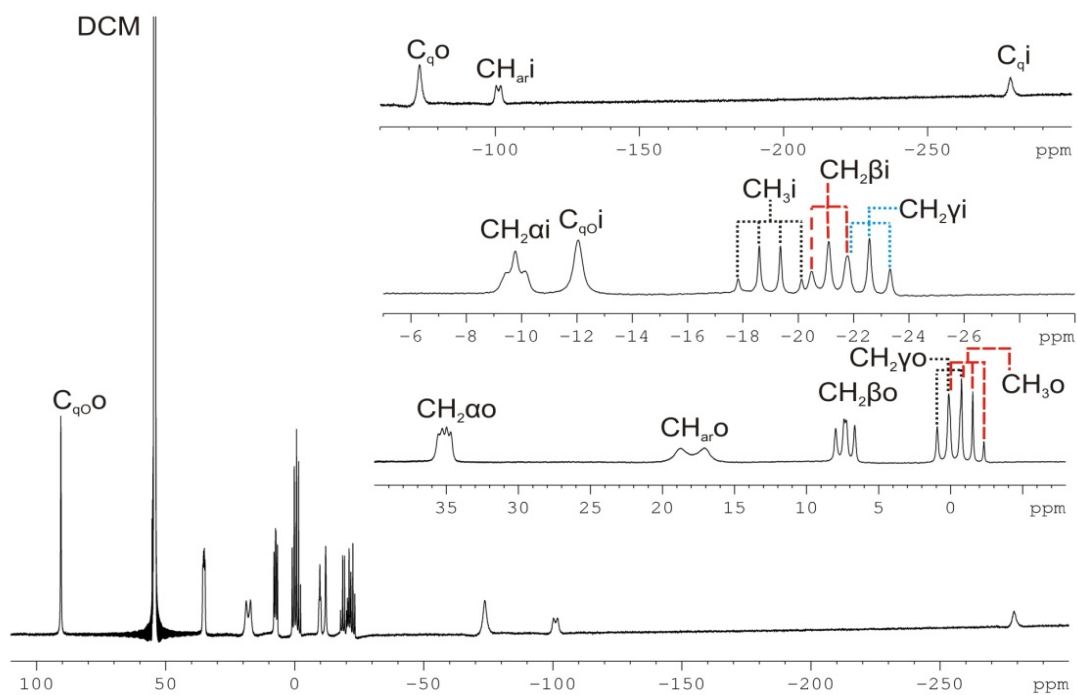


Figure S11. ^{13}C NMR spectrum of **1** dissolved in CD_2Cl_2 , with assignments. Spectrum was recorded at 14.09 T, at a temperature of 285.0 K.

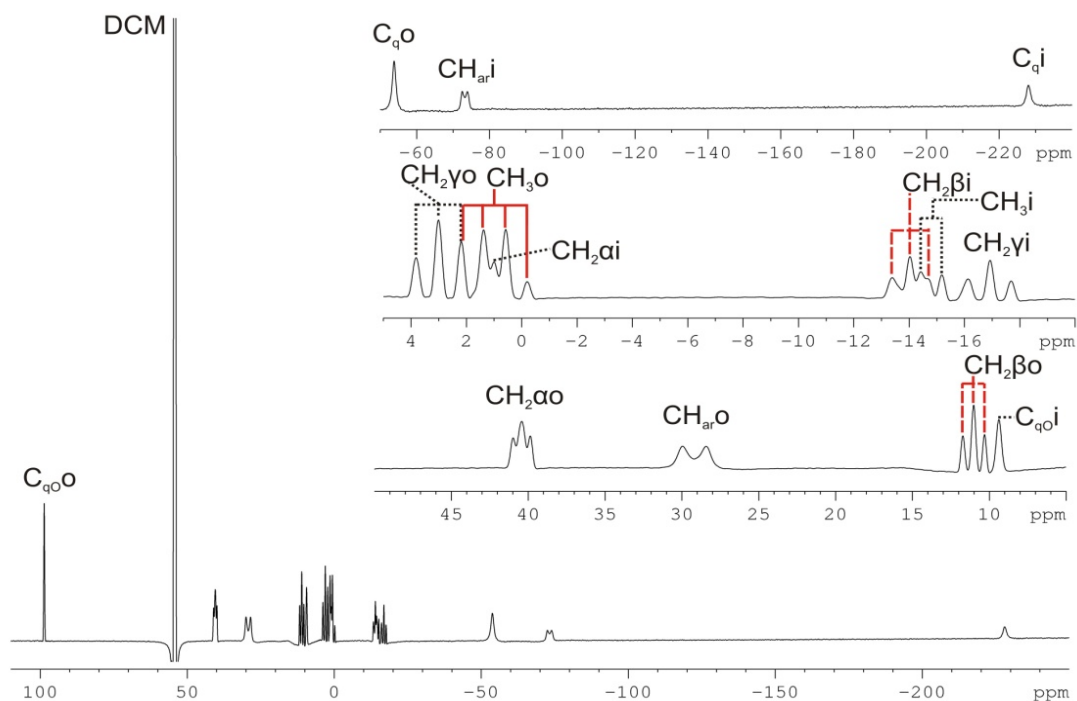


Figure S12. ^{13}C NMR spectrum of **1** dissolved in CD_2Cl_2 , with assignments. Spectrum was recorded at 14.09 T, at a temperature of 305.0 K.

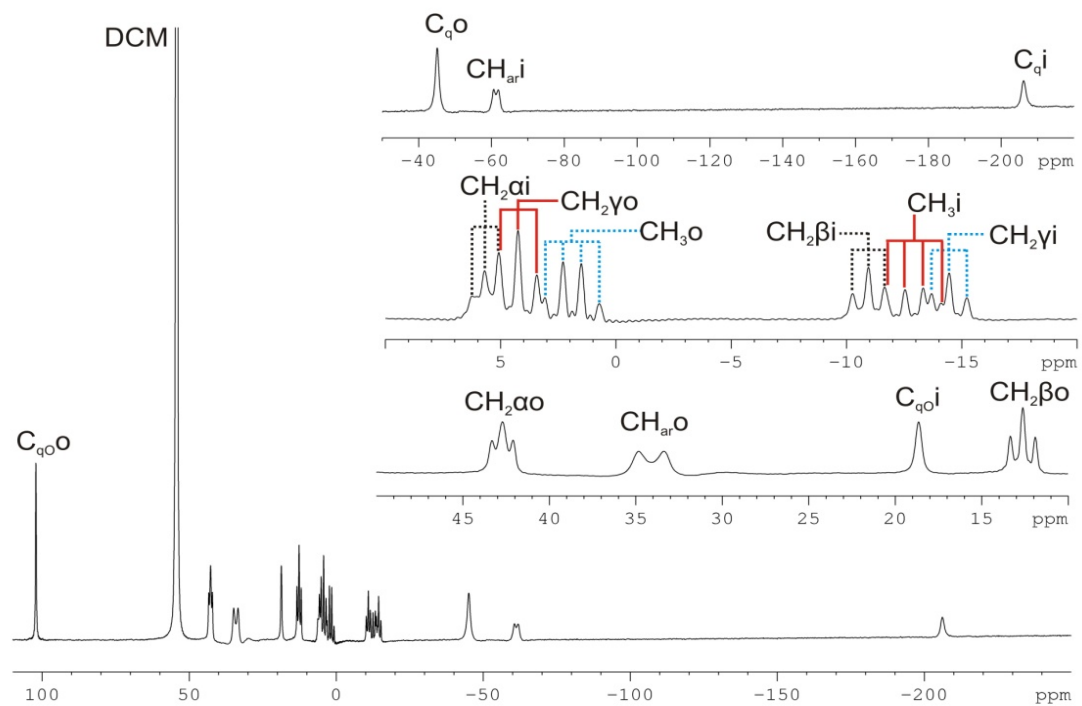


Figure S13. ^{13}C NMR spectrum of **1** dissolved in CD_2Cl_2 , with assignments. Spectrum was recorded at 14.09 T, at a temperature of at 315.0 K.

II. The model for fitting the ^{13}C NMR pseudocontact shifts (Fig. S14-S18, Table S1-S15)

Group:	Comments:	T [K]					
		265.0	275.0	285.0	295.0	305.0	315.0
		^1H NMR Data: δ_{obs} [ppm]					
CH ₂ α i		-95.93	-88.33	-81.39	-75.17	-69.58	-64.51
CH ₂ β i		-54.38	-50.40	-46.70	-43.43	-40.50	-37.82
CH ₂ γ i		-47.99	-44.33	-41.00	-38.02	-35.36	-32.92
CH ₃ i		-35.16	-32.73	-30.49	-28.47	-26.64	-24.93
CH _{ar} i		-210.86	-194.94	-180.25	-167.19	-155.53	-144.97
CH ₂ α o	1st ^1H	-24.05	-21.93	-20.04	-18.39	-16.96	-15.66
	2nd ^1H	-53.68	-48.55	-43.93	-39.87	-36.31	-33.17
CH ₂ β o	1st ^1H	-25.36	-23.25	-21.32	-19.60	-18.10	-16.74
	2nd ^1H	-26.83	-24.46	-22.31	-20.40	-18.76	-17.29
CH ₂ γ o	1st ^1H	-22.16	-20.11	-18.34	-16.82	-15.50	-14.28
	2nd ^1H	-22.16	-20.28	-18.56	-17.07	-15.76	-14.58
CH ₃ o		-16.40	-15.01	-13.78	-12.72	-11.80	-10.96
CH _{ar} o		-73.54	-67.44	-61.85	-56.90	-52.47	-48.44

Table S1. Observed ^1H NMR chemical shifts of the terbium triple decker **1** at different temperatures.

Group:	T [K]					
	265.0	275.0	285.0	295.0	305.0	315.0
	^{13}C NMR Data: δ_{obs} [ppm]					
CH ₂ α i	-23.0	-16.1	-9.8	-4.1	1.1	5.7
CH ₂ β i	-29.5	-25.2	-21.1	-17.4	-14.0	-11.0
CH ₂ γ i	-29.8	-25.9	-22.6	-19.6	-16.9	-14.5
CH ₃ i	-24.1	-21.4	-19.0	-16.7	-14.7	-13.0
C _q i	-341.0	-308.0	-278.8	-252.1	-228.1	-206.1
CH _{ar} i	-135.4	-117.2	-101.1	-86.5	-73.2	-61.2
C _q o	-38.3	-24.6	-12.1	-0.8	9.4	18.6
CH ₂ α o	28.5	32.0	35.1	37.9	40.4	42.7
CH ₂ β o	2.6	5.1	7.3	9.3	11.0	12.6
CH ₂ γ o	-3.6	-1.6	0.1	1.7	3.0	4.2
CH ₃ o	-4.0	-2.5	-1.1	0.0	1.0	1.9
C _q o	-97.7	-85.0	-73.7	-63.3	-53.8	-45.1
CH _{ar} o	5.1	11.4	17.9	23.8	29.2	34.1
C _q oO	80.6	85.8	90.6	94.8	98.6	102.1

Table S2. Observed ^{13}C NMR chemical shifts of the terbium triple decker **1** at different temperatures.

Group:	¹³ C NMR	¹ H NMR
	δ_{orb} [ppm]	
CH ₂ α i	68.7	4.06
CH ₂ β i	31.8	1.76
CH ₂ γ i	19.0	1.45
CH ₃ i	14.1	0.90
C _q i	113.8	/
CH _{ar} i	113.5	7.50
C _{qO} i	150.3	/
CH ₂ α o	68.7	4.06
CH ₂ β o	31.8	1.76
CH ₂ γ o	19.0	1.45
CH ₃ o	14.1	0.90
C _q o	113.8	/
CH _{ar} o	113.5	7.50
C _{qO} o	150.3	/

Table S3. Calculated orbital (diamagnetic) contributions to the overall ¹³C and ¹H NMR chemical shifts. Calculations were done for the phthalocyaninato ligand of complex **1** based on increments, using ChemDraw 12.¹

Group:	T [K]					
	265.0	275.0	285.0	295.0	305.0	315.0
	δ_{pc} (experimental) [ppm] = $\delta_{obs} - \delta_{orb}$					
CH ₂ α i	-91.7	-84.8	-78.5	-72.8	-67.6	-63.0
CH ₂ β i	-61.3	-57.0	-52.9	-49.2	-45.8	-42.8
CH ₂ γ i	-48.8	-44.9	-41.6	-38.6	-35.9	-33.5

Table S4. Experimental values of the ¹³C NMR pseudocontact shifts for the groups that were used in the calculation of the magnetic susceptibility anisotropy (obtained as the difference between the observed chemical shift and the calculated orbital contribution to the observed chemical shift).

Group:	r_{prox} [Å]	θ_{prox} [°]	r_{dist} [Å]	θ_{dist} [°]	$G_{prox} + G_{dist}$ [m ⁻³]	δ_{pc} [ppm]	χ_a [m ³]
CH ₂ α i	8.2519	94.65	8.7042	70.88	-2.773E+27	-72.8	9.90E-31
	8.4394	100.22	8.5473	76.34	-2.840E+27		9.66E-31
	8.7229	110.67	8.1733	86.93	-2.759E+27		9.95E-31
	8.6318	108.08	8.2481	84.17	-2.833E+27		9.69E-31
CH ₂ β i	10.1338	107.06	9.7032	86.79	-1.797E+27	-49.2	1.032E-30
	10.2277	111.74	9.5042	91.64	-1.712E+27		1.083E-30
	9.9418	99.26	10.0002	78.91	-1.828E+27		1.015E-30
	9.6262	90.90	10.1962	70.73	-1.755E+27		1.057E-30
CH ₂ γ i	10.9167	106.50	10.4754	87.73	-1.448E+27	-38.6	1.005E-30
	11.0184	105.51	10.6323	86.93	-1.412E+27		1.031E-30
	10.7536	99.20	10.7665	80.39	-1.477E+27		9.85E-31
	9.7179	82.83	10.7392	63.87	-1.376E+27		1.057E-30
Average							1.015E-30
Standard Deviation							3.7E-32

Table S5. X- ray data coordinates of the carbon atoms of the methylene groups that were used to calculate the magnetic susceptibility anisotropy of complex **1**. The table also contains the sum of the geometric factors calculated with these coordinates for both terbium centers (with equation 8 from the main text), the calculated magnetic susceptibility anisotropy for each atom in the asymmetric unit of **1**, as well as the average value of χ_a and its standard deviation. The values of δ_{pc} used in the calculation of χ_a are taken from Table S4. The asymmetric unit of complex **1** is given in Figure S31.

Group:	T [K]					
	265.0	275.0	285.0	295.0	305.0	315.0
	χ_a [m ³]					
CH ₂ α i	1.247E-30	1.152E-30	1.067E-30	9.90E-31	9.19E-31	8.57E-31
	1.217E-30	1.125E-30	1.042E-30	9.66E-31	8.97E-31	8.36E-31
	1.253E-30	1.158E-30	1.072E-30	9.95E-31	9.24E-31	8.61E-31
	1.220E-30	1.128E-30	1.045E-30	9.69E-31	9.00E-31	8.38E-31
CH ₂ β i	1.286E-30	1.196E-30	1.110E-30	1.032E-30	9.61E-31	8.97E-31
	1.350E-30	1.255E-30	1.165E-30	1.083E-30	1.01E-30	9.41E-31
	1.265E-30	1.176E-30	1.091E-30	1.015E-30	9.45E-31	8.82E-31
	1.316E-30	1.224E-30	1.136E-30	1.057E-30	9.84E-31	9.18E-31
CH ₂ γ i	1.270E-30	1.169E-30	1.083E-30	1.005E-30	9.34E-31	8.72E-31
	1.303E-30	1.199E-30	1.111E-30	1.031E-30	9.59E-31	8.94E-31
	1.246E-30	1.146E-30	1.062E-30	9.85E-31	9.16E-31	8.55E-31
	1.337E-30	1.230E-30	1.139E-30	1.057E-30	9.83E-31	9.18E-31
	Average					
	1.276E-30	1.180E-30	1.094E-30	1.015E-30	9.44E-31	8.81E-31
	Standard Deviation					
	4.3E-32	4.2E-32	3.9E-32	3.7E-32	3.5E-32	3.4E-32

Table S6. Using the coordinates from Table S5, with the experimental pseudocontact shifts given in Table S4, magnetic susceptibility anisotropy values were calculated for all temperatures at which the ¹³C and ¹H NMR spectra were recorded. The calculated χ_a values from each carbon atom in the asymmetric unit of **1**, along with the average values and standard deviations of χ_a for each temperature, are reported in this table. The χ_a values are summarized in Table S7.

T [K]	χ_a [m ³]	Standard Deviation of χ_a [m ³]
265.0	12.76E-31	0.43E-31
275.0	11.80E-31	0.42E-31
285.0	10.94E-31	0.39E-31
295.0	10.15E-31	0.37E-31
305.0	9.44E-31	0.35E-31
315.0	8.81E-31	0.34E-31

Table S7. χ_a values calculated at different temperatures from the pseudocontact shifts of the CH₂ α i, CH₂ β i and CH₂ γ i carbon atoms of **1** as described in the main text, with standard deviations.

Bond	Bond Length [Å]	Angle	Angle Value [°]
O-CH ₂ α	1.430	C _{qO} -O-CH ₂ α	117.50
CH ₂ α-CH ₂ β	1.517	O-CH ₂ α-CH ₂ β	106.50
CH ₂ β-CH ₂ γ	1.526	CH ₂ α-CH ₂ β-CH ₂ γ	113.30
CH ₂ γ-CH ₃	1.528	CH ₂ β-CH ₂ γ-CH ₃	112.90

Table S8. Bond lengths and angles used in the model made to fit the pseudocontact contributions to the overall chemical shifts of the ¹³C NMR resonances. These values were taken as average values of the corresponding bond lengths and angles measured from the crystal structure of **1** and are applied to the modeled butoxy chains of both the inner and outer phthalocyaninato ligand.

Dihedral angle φ	φ [°]	
	Inner Ligand	Outer Ligand
CH _{ar} -C _{qO} -O-CH ₂ α	0.0	23.8
C _{qO} -O-CH ₂ α-CH ₂ β	180.0	171.4
O-CH ₂ α-CH ₂ β-CH ₂ γ	180.0	177.1
CH ₂ α-CH ₂ β-CH ₂ γ-CH ₃	180.0	-172.2

Table S9. Dihedral angles describing the butoxy groups of the modeled inner and outer phthalocyaninato ligands.

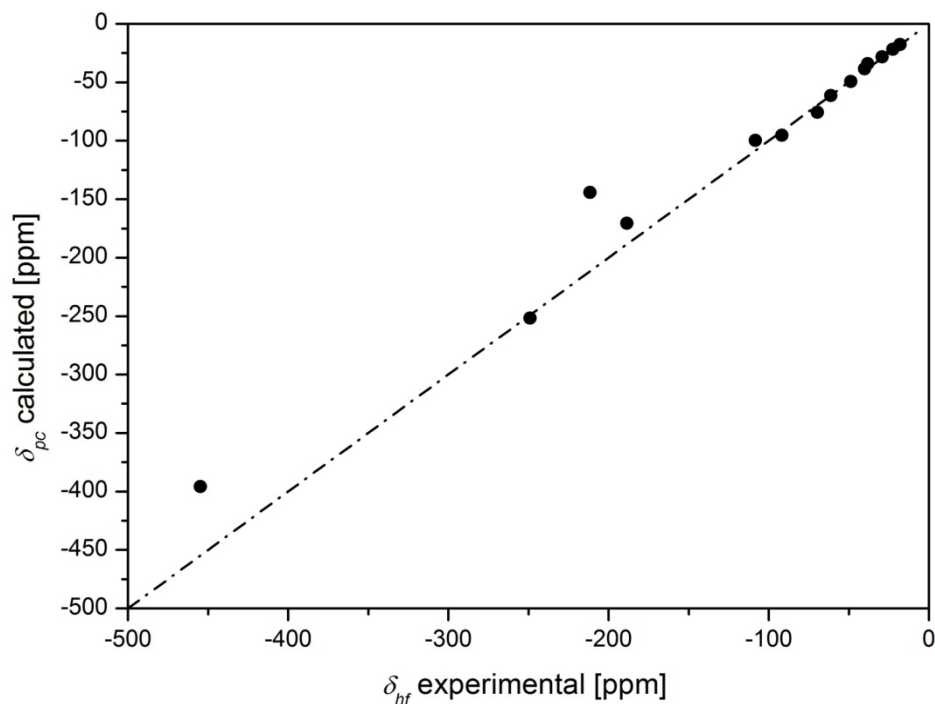


Figure S14. Calculated vs. experimental pseudocontact contributions to the overall chemical shift of the ^{13}C NMR resonances of **1** dissolved in deuterated dichloromethane at 265.0 K. The dash-dot line represents the δ_{pc} (calculated) = δ_{hf} (experimental) line.

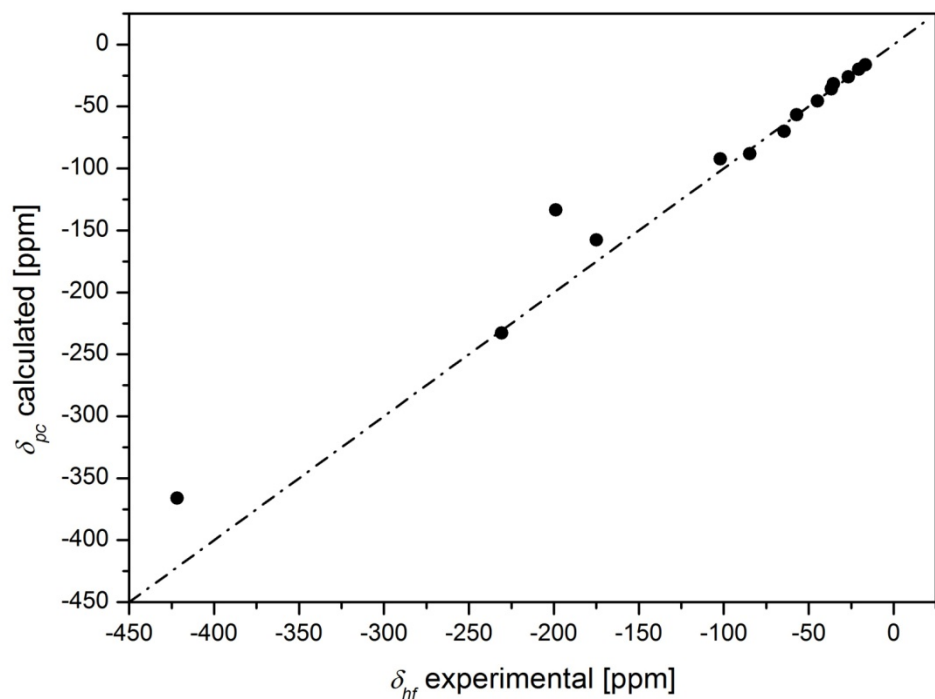


Figure S15. Calculated vs. experimental pseudocontact contributions to the overall chemical shift of the ^{13}C NMR resonances of **1** dissolved in deuterated dichloromethane at 275.0 K. The dash-dot line represents the δ_{pc} (calculated) = δ_{hf} (experimental) line.

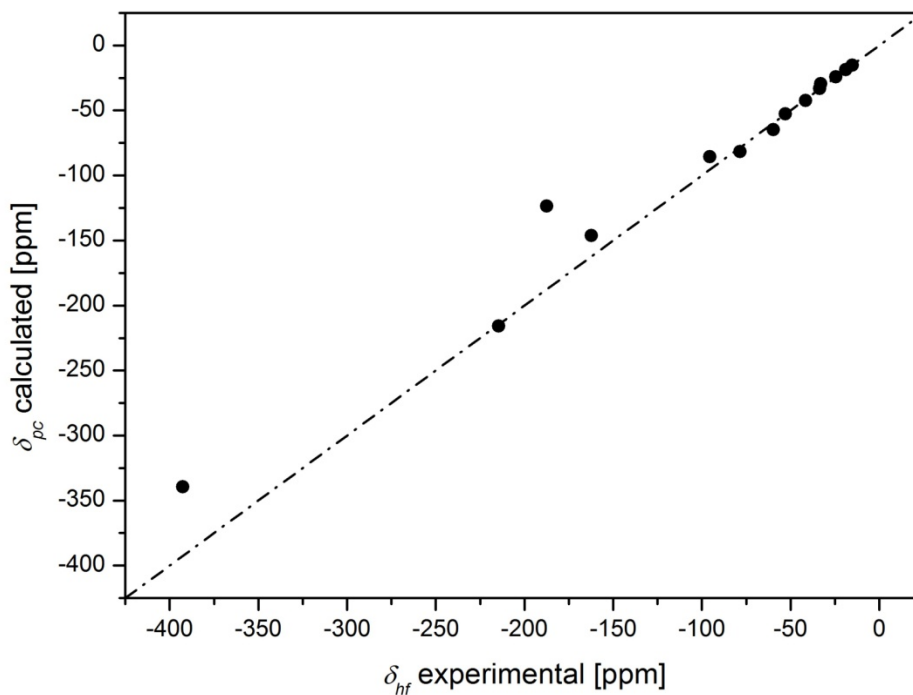


Figure S16. Calculated vs. experimental pseudocontact contributions to the overall chemical shift of the ^{13}C NMR resonances of **1** dissolved in deuterated dichloromethane at 285.0 K. The dash-dot line represents the δ_{pc} (calculated) = δ_{hf} (experimental) line.

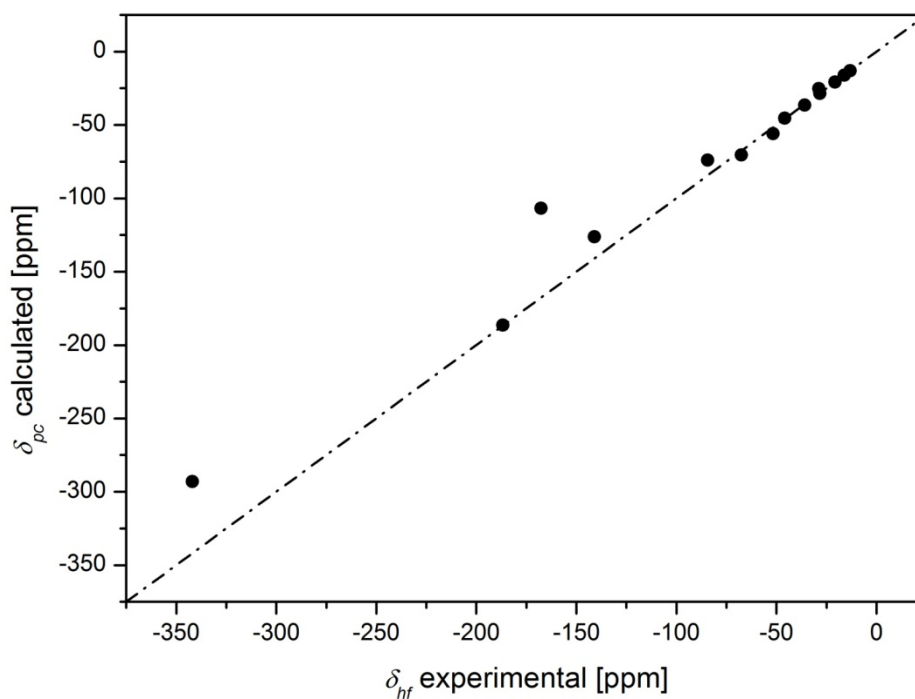


Figure S17. Calculated vs. experimental pseudocontact contributions to the overall chemical shift of the ^{13}C NMR resonances of **1** dissolved in deuterated dichloromethane at 305.0 K. The dash-dot line represents the δ_{pc} (calculated) = δ_{hf} (experimental) line.

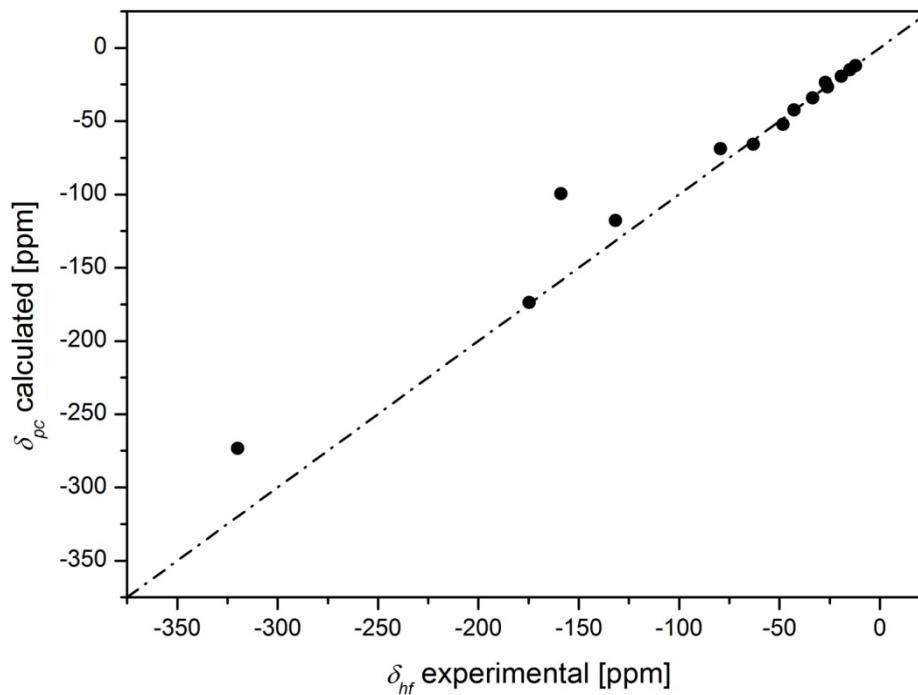


Figure S18. Calculated vs. experimental pseudocontact contributions to the overall chemical shift of the ^{13}C NMR resonances of **1** dissolved in deuterated dichloromethane at 315.0 K. The dash-dot line represents the δ_{pc} (calculated) = δ_{hf} (experimental) line.

Group:	r_{prox} [Å]	θ_{prox} [°]	r_{dist} [Å]	θ_{dist} [°]
CH ₂ αi	8.5242	101.90	8.5242	78.10
CH ₂ βi	10.0068	100.11	10.0068	79.89
CH ₂ γi	10.8030	99.37	10.8030	80.63
CH ₃ i	12.2812	98.23	12.2812	81.77
C _q i	4.5561	112.70	4.5561	67.30
CH _{ar} i	5.7945	107.66	5.7945	72.34
C _{qO} i	6.8255	104.93	6.8255	75.07
CH ₂ αo	8.6244	73.35	10.2042	54.07
CH ₂ βo	10.1208	74.36	11.5760	57.34
CH ₂ γo	10.9806	73.36	12.4520	57.66
CH ₃ o	12.4400	75.00	13.7753	60.73

Table S10. Coordinates of the modeled ^{13}C nuclei of the inner and outer phthalocyaninato ligands.

Group:	Comments:	T [K]					
		265.0		275.0		285.0	
		δ_{pc} calc. [ppm]	δ_{hf} exptl. ^{a)} [ppm]	δ_{pc} calc. [ppm]	δ_{hf} exptl. ^{a)} [ppm]	δ_{pc} calc. [ppm]	δ_{hf} exptl. ^{a)} [ppm]
CH ₂ α i		-95.3	-91.7	-88.2	-84.8	-81.7	-78.5
CH ₂ β i		-61.3	-61.3	-56.7	-57.0	-52.5	-52.9
CH ₂ γ i		-49.4	-48.8	-45.7	-44.9	-42.4	-41.6
CH ₃ i		-34.3	-38.2	-31.7	-35.5	-29.4	-33.1
C _{q0} i		-170.5	-188.6	-157.6	-174.9	-146.1	-162.3
CH _{ar} i		-251.8	-248.9	-232.8	-230.7	-215.8	-214.6
C _q i		-395.9	-454.8	-366.1	-421.8	-339.4	-392.6
CH ₂ α o		-38.7	-40.2	-35.8	-36.7	-33.2	-33.6
CH ₂ β o		-28.3	-29.2	-26.1	-26.7	-24.2	-24.5
CH ₂ γ o		-21.8	-22.6	-20.1	-20.6	-18.6	-18.9
CH ₃ o		-17.7	-18.1	-16.4	-16.6	-15.2	-15.2
C _{q0} o	XRD ^{b)}	-75.7	-69.7	-70.0	-64.5	-64.9	-59.7
CH _{ar} o	XRD ^{b)}	-99.9	-108.4	-92.4	-102.1	-85.6	-95.6
C _q o	XRD ^{b)}	-144.2	-211.5	-133.4	-198.8	-123.6	-187.5

Table S11. Calculated pcs from model (δ_{pc} calc.) vs. experimental hyperfine contributions to the overall observed chemical shifts in (δ_{hf} exptl.) ¹³C NMR spectra of **1** dissolved in CD₂Cl₂ at temperatures 265.0 K – 285.0 K. a) The values of the experimental hyperfine shifts mentioned here correspond to the differences between the observed chemical shifts and the diamagnetic contributions to these chemical shifts. b) The pseudocontact shift for the indicated group was calculated as the average value of the pseudocontact shifts of the eight individual carbon atoms of this group (see asymmetric unit, Figure S31).

Group:	Comments:	T [K]					
		295.0		305.0		315.0	
		δ_{pc} calc. [ppm]	δ_{hf} exptl. ^{a)} [ppm]	δ_{pc} calc. [ppm]	δ_{hf} exptl. ^{a)} [ppm]	δ_{pc} calc. [ppm]	δ_{hf} exptl. ^{a)} [ppm]
CH ₂ α i		-75.9	-72.8	-70.6	-67.6	-65.8	-63.0
CH ₂ β i		-48.8	-49.2	-45.4	-45.8	-42.3	-42.8
CH ₂ γ i		-39.3	-38.6	-36.6	-35.9	-34.1	-33.5
CH ₃ i		-27.3	-30.8	-25.4	-28.8	-23.7	-27.1
C _q Oi		-135.7	-151.1	-126.2	-140.9	-117.7	-131.7
CH _{ar} i		-200.4	-200.0	-186.3	-186.7	-173.8	-174.7
C _q i		-315.1	-365.9	-293.0	-341.9	-273.3	-319.9
CH ₂ α o		-30.8	-30.8	-28.6	-28.3	-26.7	-26.0
CH ₂ β o		-22.5	-22.5	-20.9	-20.8	-19.5	-19.2
CH ₂ γ o		-17.3	-17.3	-16.1	-16.0	-15.0	-14.8
CH ₃ o		-14.1	-14.1	-13.1	-13.1	-12.2	-12.2
C _q Oo	XRD ^{b)}	-60.3	-55.5	-56.0	-51.7	-52.3	-48.2
CH _{ar} o	XRD ^{b)}	-79.5	-89.7	-73.9	-84.3	-69.0	-79.4
C _q o	XRD ^{b)}	-114.8	-177.1	-106.8	-167.6	-99.6	-158.9

Table S12. Calculated *pcs* from model (δ_{pc} calc.) vs. experimental hyperfine contributions to the overall observed chemical shifts (δ_{hf} exptl.) in ¹³C NMR spectra of **1** dissolved in CD₂Cl₂ at temperatures 295.0 K – 315.0 K. a) The values of the experimental hyperfine shifts mentioned here correspond to the differences between the observed chemical shifts and the orbital contributions to these chemical shifts. b) The pseudocontact shift for the indicated group was calculated as the average value of the pseudocontact shifts of the eight individual carbon atoms of this group (see asymmetric unit, Figure S31).

C _q O				
Atom:	r_{prox} [Å]	θ_{prox} [°]	r_{dist} [Å]	θ_{dist} [°]
1	4.4457	73.91	6.3869	41.98
2	4.4366	74.69	6.3463	42.39
3	4.5195	67.61	6.7006	38.58
4	4.4986	69.07	6.6262	39.35
5	4.5654	65.59	6.8172	37.58
6	4.5627	65.35	6.8241	37.34
7	4.4824	71.56	6.5136	40.76
8	4.5249	69.57	6.6295	39.76
CH _{ar} O				
Atom:	r_{prox} [Å]	θ_{prox} [°]	r_{dist} [Å]	θ_{dist} [°]
1	5.7887	72.85	7.6076	46.64
2	5.8020	70.65	7.7168	45.19
3	5.8635	68.14	7.8802	43.68
4	5.8479	68.63	7.8455	43.96
5	5.8239	72.25	7.6661	46.35
6	5.7477	75.94	7.4311	48.62
7	5.6676	79.81	7.1791	50.99
8	5.7221	78.10	7.3080	50.01
C _q O ₀				
Atom:	r_{prox} [Å]	θ_{prox} [°]	r_{dist} [Å]	θ_{dist} [°]
1	6.8167	72.88	8.5406	49.71
2	6.8128	73.76	8.4960	50.34
3	6.8880	69.46	8.7638	47.39
4	6.8928	69.27	8.7770	47.26
5	6.7887	76.72	8.3320	52.46
6	6.8334	75.00	8.4555	51.32
7	6.7081	81.25	8.0339	55.62
8	6.6747	82.17	7.9566	56.21

Table S13. Coordinates of the C_qO, CH_{ar}O and C_qO₀ carbon atoms, as taken from the asymmetric unit of complex **1** (Figure S31).

Atom:	T [K]					
	265.0	275.0	285.0	295.0	305.0	315.0
	C _{qO} : δ_{pc} (calculated) [ppm]					
1	-211.0	-195.1	-180.8	-167.9	-156.1	-145.6
2	-222.2	-205.5	-190.5	-176.9	-164.5	-153.4
3	-113.3	-104.8	-97.1	-90.2	-83.8	-78.2
4	-137.0	-126.7	-117.5	-109.1	-101.4	-94.6
5	-79.0	-73.1	-67.7	-62.9	-58.5	-54.5
6	-74.9	-69.2	-64.2	-59.6	-55.4	-51.7
7	-174.7	-161.5	-149.7	-139.0	-129.3	-120.6
8	-141.9	-131.3	-121.7	-113.0	-105.0	-98.0
Average	-144.2	-133.4	-123.6	-114.8	-106.8	-99.6
Standard Deviation	55.5	51.3	47.6	44.2	41.1	38.3
	CH _{arO} : δ_{pc} (calculated) [ppm]					
1	-97.2	-89.8	-83.3	-77.3	-71.9	-67.1
2	-80.1	-74.1	-68.7	-63.7	-59.3	-55.3
3	-58.7	-54.3	-50.3	-46.7	-43.4	-40.5
4	-62.9	-58.2	-53.9	-50.1	-46.6	-43.4
5	-91.3	-84.4	-78.3	-72.7	-67.6	-63.0
6	-121.0	-111.9	-103.7	-96.3	-89.6	-83.5
7	-151.2	-139.8	-129.6	-120.3	-111.9	-104.4
8	-136.8	-126.5	-117.3	-108.9	-101.3	-94.5
Average	-99.9	-92.4	-85.6	-79.5	-73.9	-69.0
Standard Deviation	33.8	31.2	28.9	29.6	25.0	23.3
	C _{qOO} : δ_{pc} (calculated) [ppm]					
1	-65.3	-60.3	-55.9	-51.9	-48.3	-45.1
2	-69.7	-64.4	-59.7	-55.4	-51.6	-48.1
3	-46.5	-43.0	-39.8	-37.0	-34.4	-32.1
4	-45.4	-42.0	-38.9	-36.1	-33.6	-31.3
5	-84.4	-78.0	-72.3	-67.2	-62.5	-58.3
6	-75.1	-69.5	-64.4	-59.8	-55.6	-51.9
7	-107.1	-99.1	-91.8	-85.3	-79.3	-74.0
8	-112.3	-103.9	-96.3	-89.4	-83.1	-77.5
Average	-75.7	-70.0	-64.9	-60.3	-56.0	-52.3
Standard Deviation	24.9	23.0	21.3	19.8	18.4	17.2

Table S14. Calculated pseudocontact shift contributions to the hyperfine shift of the C_{qO}, CH_{arO} and C_{qOO} ¹³C NMR resonances at temperatures 265.0 K – 315.0 K, as calculated with the coordinates from Table S13. CD₂Cl₂ was used as solvent.

T [K]	C_{qOo}	CH_{arO}	C_{qO}	C_{qOi}	CH_{arI}	C_{qI}
	δ_{fc} [ppm]					
265.0	6.0 (24.9)	-8.5 (33.8)	-67.3 (55.5)	-18.1	2.9	-58.9
275.0	5.5 (23.0)	-9.7 (31.2)	-65.4 (51.3)	-17.2	2.1	-55.7
285.0	5.2 (21.3)	-10.0 (28.9)	-63.9 (47.6)	-16.2	1.2	-53.2
295.0	4.8 (19.8)	-10.2 (26.9)	-62.3 (44.2)	-15.4	0.4	-50.8
305.0	4.4 (18.4)	-10.4 (25.0)	-60.9 (41.1)	-14.7	-0.4	-48.9
315.0	4.1 (17.2)	-10.4 (23.3)	-59.3 (38.3)	-14.0	-0.9	-46.6

Table S15. Contributions to the hyperfine shift that can be attributed to the Fermi-contact interaction, obtained from ^{13}C NMR spectra recorded at different temperatures. These were calculated as the difference between the pseudocontact shifts calculated from the model and the pseudocontact shifts obtained from the experiment. Standard deviations are given in brackets. Since the groups of the inner phthalocyaninato ligand were modeled, no standard deviations could be calculated for these.

III. ^1H and ^{13}C NMR spectra of complex **1** in toluene- d^8 (Fig. S19-S21, Table S16-S17)

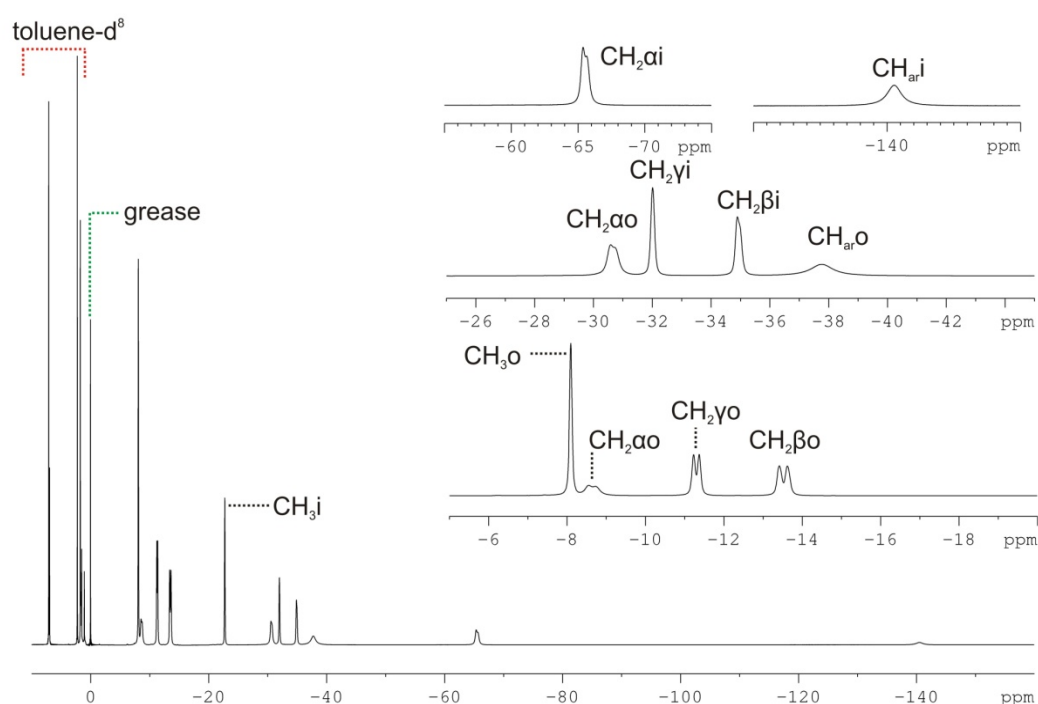


Figure S19. ^1H NMR spectrum of **1** dissolved in toluene- d^8 , with assignments. Spectrum was recorded at 14.09 T, at a temperature of 295.0 K.

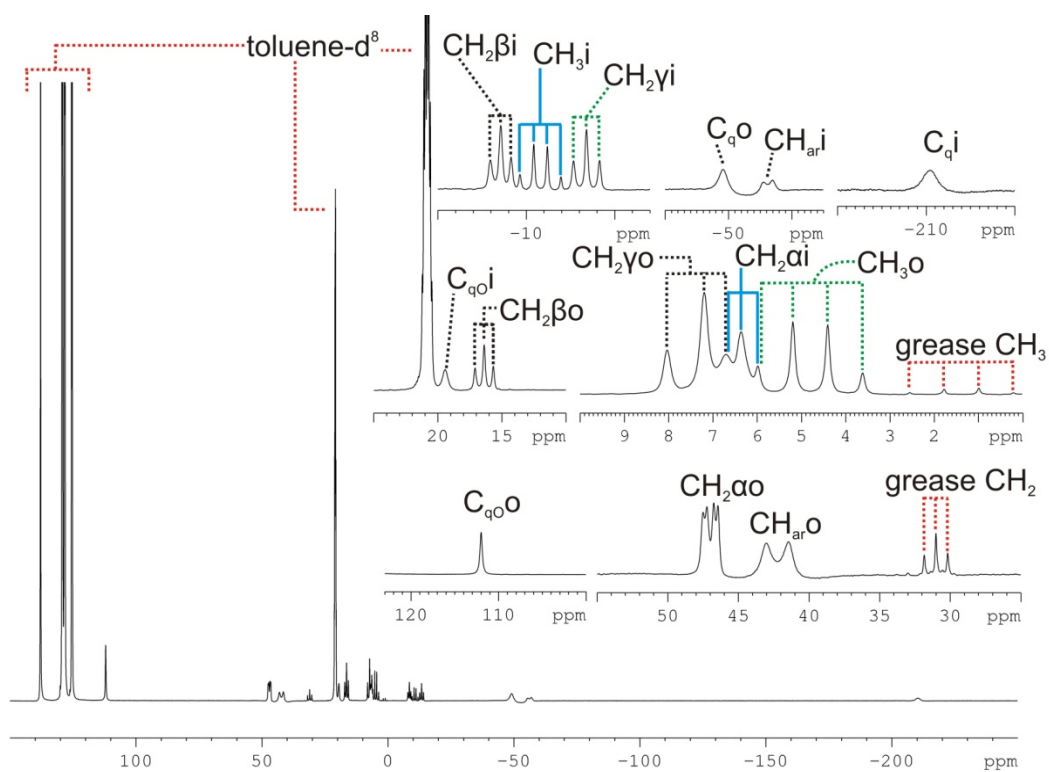


Figure S20. ^{13}C NMR spectrum of **1** dissolved in toluene- d^8 , with assignments. Spectrum was recorded at 14.09 T, at a temperature of 295.0 K.

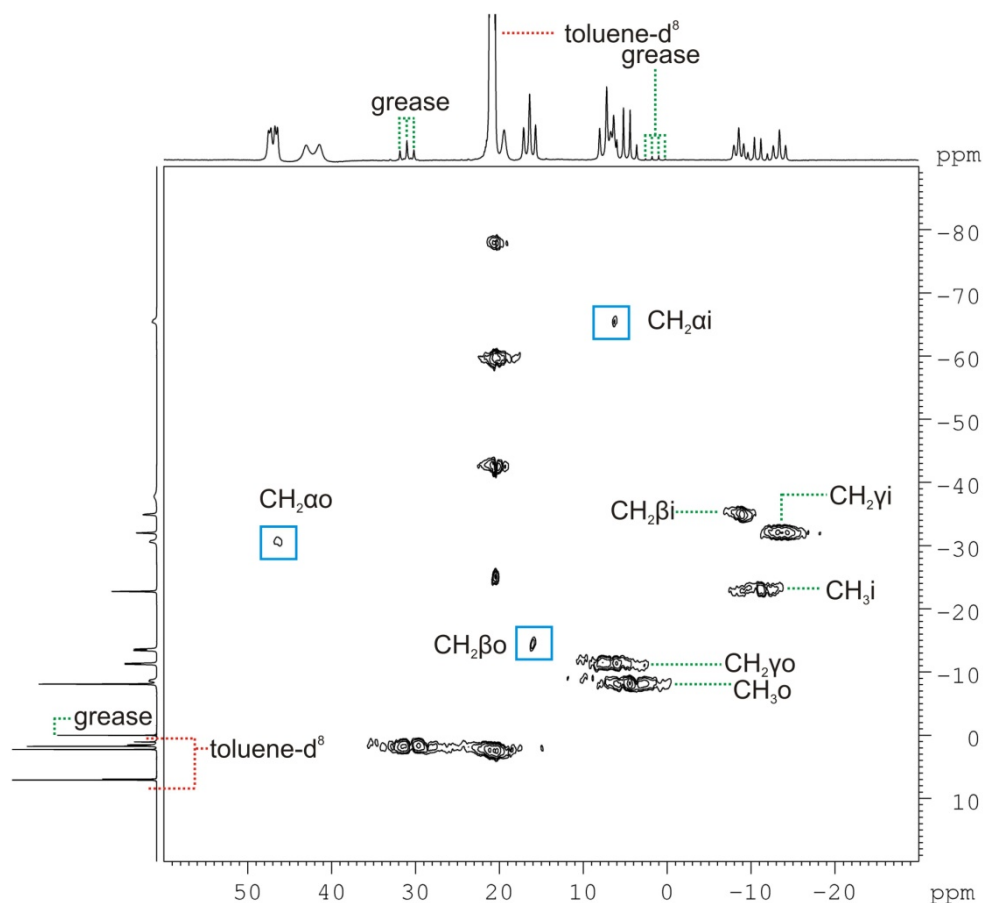


Figure S21. ^1H , ^{13}C NMR correlation spectrum (HETCOR, ^{13}C in F2, horizontal) of compound **1** dissolved in toluene- d^8 , recorded at 14.09 T, at a temperature of 295.0 K. The crosspeaks of all the aliphatic groups are present. The assignments of aromatic resonances, that did not show crosspeaks in this experiment due to their fast relaxation, were made based on the values of their observed chemical shifts.

Group:	δ_{obs} in ^1H NMR [ppm]	δ_{obs} in ^{13}C NMR [ppm]
$\text{CH}_2\alpha\text{i}$	-65.53	6.3
$\text{CH}_2\beta\text{i}$	-34.94	-8.6
$\text{CH}_2\gamma\text{i}$	-32.01	-13.4
CH_3i	-22.72	-10.8
$\text{C}_{\text{q}}\text{i}$	/	-210.3
$\text{CH}_{\text{ar}}\text{i}$	-140.98	-56.2
$\text{C}_{\text{q}}\text{o}\text{i}$	/	19.4
$\text{CH}_2\alpha\text{o}$	-8.64; -30.63	47.0
$\text{CH}_2\beta\text{o}$	-13.51	16.4
$\text{CH}_2\gamma\text{o}$	-11.30	7.2
CH_3o	-8.09	4.8
$\text{C}_{\text{q}}\text{o}$	/	-49.2
$\text{CH}_{\text{ar}}\text{o}$	-37.73	42.2
$\text{C}_{\text{q}}\text{o}\text{o}$	/	112.0

Table S16. Observed ^1H and ^{13}C NMR chemical shifts (δ_{obs}) of **1** dissolved in toluene- d^8 at 295.0 K.

		$T = 295.0 \text{ K}$	
Group:	Comments:	δ_{pc} calc. [ppm]	δ_{hf} exptl. ^{a)} [ppm]
CH ₂ α i		-63.6	-62.4
CH ₂ β i		-40.9	-40.4
CH ₂ γ i		-33.0	-32.4
CH ₃ i		-22.9	-24.9
C _q o <i>i</i>		-113.8	-130.9
CH _{ar} i		-168.1	-169.7
C _q i		-264.3	-324.1
CH ₂ α o		-25.8	-21.7
CH ₂ β o		-18.9	-15.4
CH ₂ γ o		-14.5	-11.8
CH ₃ o		-11.8	-9.3
C _q o <i>o</i>	XRD ^{b)}	-50.5	-38.3
CH _{ar} o	XRD ^{b)}	-66.7	-71.3
C _q o	XRD ^{b)}	-96.3	-163.0

Table S17. Calculated pcs from model (δ_{pc} calc.) vs. experimental hyperfine contributions to the overall observed chemical shifts (δ_{hf} exptl.) in ¹³C NMR spectra of **1** dissolved in toluene-d⁸ at a temperature of 295.0 K. a) The values of the experimental hyperfine shifts mentioned here correspond to the differences between the observed chemical shifts and the diamagnetic contributions to the chemical shifts. b) The pseudocontact shift for the indicated group was calculated as the average value of the pseudocontact shifts of the eight individual carbon atoms of this group (see asymmetric unit, Figure S31).

IV. Isointensity plots and estimated pseudocontact shifts (Eq. S1-S6, Fig. S22-S23, Table S18-S19)

The carbon atoms present in Figure 6 possess the same coordinates as those that were used in our model. The coordinates of aromatic carbon atoms of the outer ring were averaged from X-ray data (Table S13).

For a single terbium ion in a complex that has a magnetic anisotropy susceptibility value whose magnitude is 50% of the χ_a value of complex **1** at 295 K, drawing an isointensity plot represents a trivial task of calculating the distance between a nucleus N and the terbium ion for all values of the θ angle, ranging from 0° to 360°, that would give a certain pseudocontact shift. An isointensity plot for such a complex would appear as in Figure S22, with the metal center at the origin of the coordinate

system. The borderline region where the sign of the pseudocontact shift changes corresponds to a θ angle of 54.7356° .

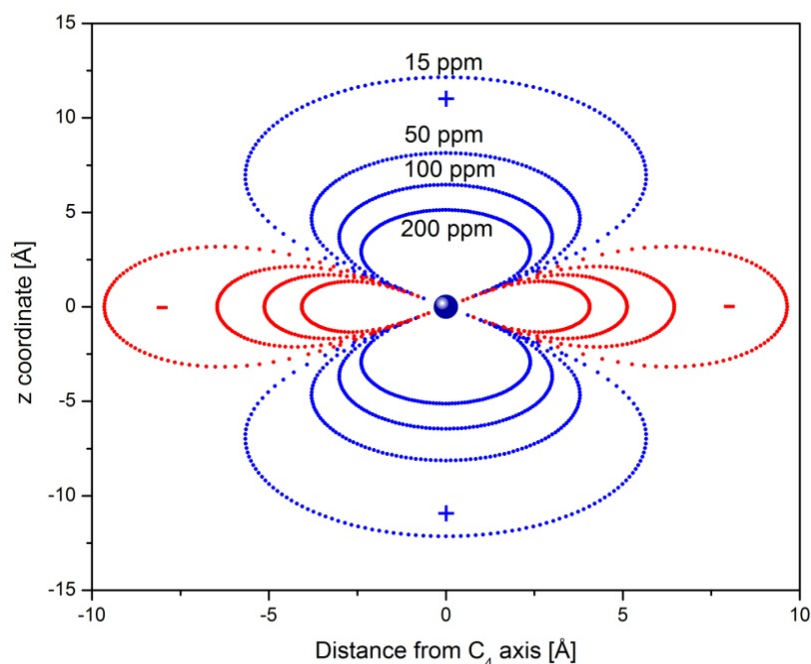


Figure S22. Isointensity plots of a complex with a single Terbium ion and a χ_a value equal to 50% of that calculated for complex **1** dissolved in deuterated dichloromethane at 295.0 K. The values of the pseudocontact shifts are indicated, with positive values painted blue and marked with a plus sign, while negative values are painted red and marked with a minus sign. The single terbium ion is represented with a sphere of deep blue color.

In the approach to calculate the isointensity plots of complex **1**, the origin of a coordinate system was placed exactly between the two metal centers, on the molecular z axis (passing through both terbium ions, coincidental with the magnetic field axis). For a given distance along the z axis and a given distance away from the z axis (on the x axis), the (Z, X) coordinates can be used to fully describe a position of a nucleus relative to the two terbium ions, since the distance between these metal centers is known from the XRD data. For a nucleus with coordinates (Z, X) in this coordinate system, the corresponding distances from the proximal and distal terbium ions, as well as the angles between the nucleus-terbium ion vectors and the magnetic field (z axis) vector, can be obtained by using the following equations S1-S6:

$$r_{prox,z} = \left| (d_{Tb-Tb}/2) - kZ \right| \quad (S1)$$

$$r_{dist,z} = \left| (d_{Tb-Tb}/2) - mZ \right| \quad (S2)$$

$$r_{prox} = \sqrt{r_{prox,Z}^2 + X^2} \quad (S3)$$

$$r_{dist} = \sqrt{r_{dist,Z}^2 + X^2} \quad (S4)$$

$$\theta_{dist} = \arcsin(X / r_{dist}) \quad (S5)$$

$$\theta_{prox} = \arcsin(X / r_{prox}) \quad (S6)$$

Where Z is the distance from the origin along the z axis, k is +1 for Z larger than zero and -1 for Z smaller than zero, m is -1 for Z larger than zero and +1 for Z smaller than zero, X denotes the distance of nucleus N from the z axis, $r_{prox,Z}$ is the distance between nucleus N and the proximal terbium ion only along the z axis, $r_{dist,Z}$ is the distance between nucleus N and the distal terbium ion only along the z axis (note that in this coordinate system the proximal terbium is the one with a positive value on the z axis and the distal terbium has a negative value on the z axis), d_{Tb-Tb} is the XRD distance between the two metal centers, r_{prox} is the absolute distance between nucleus N at coordinates (Z, X) and the proximal terbium ion, r_{dist} is the absolute distance between the same nucleus N and the distal terbium ion, θ_{prox} and θ_{dist} are the angles between the nucleus N-Tb vectors and z axis for the proximal and distal terbium ions, respectively. The equations above relate r_{prox} , r_{dist} , θ_{prox} and θ_{dist} (from equation 8) to a two dimensional coordinate system with an origin placed at the center of the complex.

Distances from the origin along the z axis, ranging from -10.0 to 10.0 Å were generated (with increments of 0.1 Å). The objective was to find a distance X away from the z axis that would, when utilized in equations S1-S6, lead to a calculated value of the pseudocontact shift that matches a pre-set value. This approach enables an isointensity plot to be produced by having one variable only, i.e. X , for a given value of Z . The fastest way to find the satisfactory values of X was by using iterations.

The Microsoft Visual Basic code for the Excel Macro used for producing isointensity plots is given here:

```
Sub solver_iteration()
Dim count
For count = 10 To 210
SolverOk SetCell:="$S$" & count, MaxMinVal:=3, ValueOf:="200", _
ByChange:="$J$" & count
SolverOptions MaxTime:=100, Iterations:=100, Precision:=0.001, AssumeLinear:= _
False, StepThru:=False, Estimates:=1, Derivatives:=1, SearchOption:=1, _
IntTolerance:=5, Scaling:=False, Convergence:=0.001, AssumeNonNeg:=False
SolverOk SetCell:="$S$" & count, MaxMinVal:=3, ValueOf:="200", _
ByChange:="$J$" & count
SolverSolve True
Next
End Sub
```

The chemical shift value to be calculated (in ppm) is to be inserted as the "ValueOf" parameter. The code then searches for a best value of X (located in column J), that would make the absolute values in

column S equal to the sought after pseudocontact shift value (hence also enabling a negative value to be calculated for the pseudocontact shift). Only values of X that ultimately gave a match between the “ValueOf” parameter and the absolute value of the corresponding chemical shift in column S were kept and plotted on both sides of the x axis in Figure 6 of the main text. This procedure was repeated for each of the 200 generated distances along the z axis (that in this case occupied rows 10 to 210). It is interesting to mention that, when utilizing the approach above to find values of X that would lead to a pseudocontact shift of 10000 ppm, the isointensity plot shows a region where the pseudocontact shifts are positive between the two terbium ions, i.e. at close distances to the terbium ions, the individual effects of each one of them can be observed. This roughly resembles two isointensity plots of single terbium ions being brought together and overlapping. This isointensity plot is given in Figure S23.

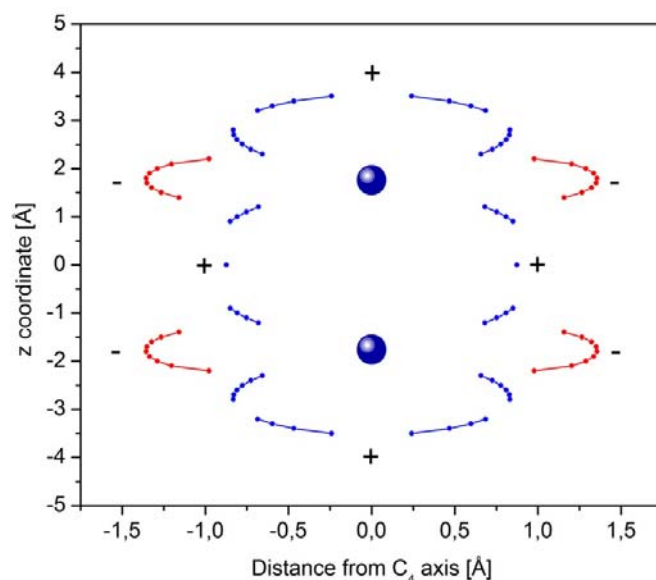


Figure S23. Isointensity plot of **1** at 295.0 K for the extreme case of a pseudocontact shift of 10000 ppm. Positive pseudocontact shift values are painted blue and marked with a plus sign, while negative values are painted red and marked with a minus sign. Terbium ions are represented by the two spheres colored in deep blue. The magnetic susceptibility anisotropy value used in this calculation was derived from the ^{13}C NMR spectrum of **1** dissolved in CD_2Cl_2 .

Isointensity plots have previously been used for the study of ^1H NMR spectra of mononuclear and dinuclear phthalocyanine based lanthanide complexes by Ishikawa et al.ⁱⁱ

Atom:	C _{No}				
	r_{prox} [Å]	θ_{prox} [°]	r_{dist} [Å]	θ_{dist} [°]	δ_{pc} at 295.0 K [ppm]
1	3.3400	63.71	5.8240	30.94	-132.9
2	3.2750	67.13	5.6600	32.21	-248.9
3	3.3500	61.83	5.8920	30.09	-73.4
4	3.3500	61.03	5.9160	29.70	-47.8
5	3.3260	61.98	5.8670	30.03	-80.8
6	3.3010	64.92	5.7450	31.31	-176.2
7	3.2800	67.20	5.6590	32.33	-249.7
8	3.2720	69.57	5.6120	32.87	-317.7
Average	3.2948	65.92	5.7208	31.64	-206.1
Standard Deviation	0.0242	3.24	0.1120	1.25	101.6

Table S18. Coordinates of the C_{No} carbon atoms, as taken from the asymmetric unit of the crystal structure of **1** (Figure S31), and the calculated pseudocontact shift contributions to the hyperfine shift of the C_{No} resonance at 295.0 K, calculated with these coordinates. Applies for **1** dissolved in CD₂Cl₂. C_{No} was not observed experimentally.

Atom:	C _{Ni}				
	r_{prox} [Å]	θ_{prox} [°]	r_{dist} [Å]	θ_{dist} [°]	δ_{pc} at 295.0 K [ppm]
1	3.5346	122.81	3.3746	61.68	-300.2
2	3.5113	121.96	3.4092	60.91	-296.8
3	3.4376	120.14	3.4705	58.94	-291.5
4	3.3709	118.22	3.5380	57.08	-300.7
Average	3.4636	120.78	3.4481	59.65	-297.3
Standard Deviation	0.0743	2.04	0.0719	2.07	4.3

Table S19. Coordinates of the C_{Ni} carbon atoms, as taken from the asymmetric unit of the crystal structure of **1** (Figure S31), and the calculated pseudocontact shift contributions to the hyperfine shift of the C_{Ni} resonance at 295.0 K, calculated with these coordinates. Applies for **1** dissolved in CD₂Cl₂. C_{Ni} was not observed experimentally.

V. ^1H NMR *pcs* according to the model established for fitting the ^{13}C NMR data (Table S20-S22)

Group:	Comments:	r_{prox} [Å]	θ_{prox} [°]	r_{dist} [Å]	θ_{dist} [°]
$\text{CH}_2\alpha_i$		8.0101	96.14	8.3965	71.53
$\text{CH}_2\beta_i$		10.2208	94.86	10.5233	75.41
$\text{CH}_2\gamma_i$		10.5039	94.73	10.7985	75.79
		12.4587	93.94	12.7105	77.92
CH_3_i		12.8675	97.93	12.8627	82.22
		12.7024	102.00	12.4554	85.97
CH_{ar}_i		6.1329	106.66	6.1329	73.34
$\text{CH}_2\alpha_o$	farther $^1\text{H}^a$)	8.4574	66.41	10.3775	48.32
	closer $^1\text{H}^a$)	8.3113	78.25	9.6616	57.38
$\text{CH}_2\beta_o$	farther $^1\text{H}^a$)	10.5303	70.38	12.1706	54.59
	closer $^1\text{H}^a$)	10.4017	79.91	11.5489	62.47
$\text{CH}_2\gamma_o$	farther $^1\text{H}^a$)	11.0160	67.97	12.7584	53.17
	closer $^1\text{H}^a$)	10.6999	76.94	11.9939	60.35
CH_3_o	1st ^1H	12.8547	72.03	14.3353	58.54
	2nd ^1H	13.0584	74.45	14.4052	60.85
	3rd ^1H	12.5778	79.73	13.6507	65.04

Table S20. Coordinates of the ^1H nuclei, according to the created model of the inner and outer phthalocyaninato ligands. Because of the symmetry restriction of the inner ring, coordinates for only one of the two ^1H nuclei of the inner alkyl chain are needed in further calculations. a) For the methylene groups of the outer phthalocyaninato ligand, the protons are also distinguished in this table by qualitatively describing them as further away from or closer to the two terbium centers of the complex.

Group:	Comments:	T [K]					
		265.0		275.0		285.0	
		δ_{pc} calc. [ppm]	δ_{hf} exptl. ^{b)} [ppm]	δ_{pc} calc. [ppm]	δ_{hf} exptl. ^{b)} [ppm]	δ_{pc} calc. [ppm]	δ_{hf} exptl. ^{b)} [ppm]
CH ₂ α i		-103.55	-99.99	-95.75	-92.39	-88.76	-85.45
CH ₂ β i		-54.53	-56.14	-50.42	-52.16	-46.74	-48.46
CH ₂ γ i		-50.62	-49.44	-46.81	-45.78	-43.39	-42.45
CH ₃	1st ¹ H	-31.57	-36.06	-29.19	-33.63	-27.06	-31.39
	2nd ¹ H	-30.01	-36.06	-27.75	-33.63	-25.72	-31.39
	3rd ¹ H	-31.62	-36.06	-29.24	-33.63	-27.11	-31.39
	average	-31.07	-36.06	-28.73	-33.63	-26.63	-31.39
CH _{ar} i		-221.07	-218.36	-204.43	-202.44	-189.50	-187.75
CH ₂ α o	farther ¹ H ^{a)}	-19.19	-28.11	-17.74	-25.99	-16.45	-24.10
	closer ¹ H ^{a)}	-56.41	-57.74	-52.17	-52.61	-48.36	-47.99
CH ₂ β o	farther ¹ H ^{a)}	-19.04	-27.12	-17.61	-25.01	-16.32	-23.08
	closer ¹ H ^{a)}	-35.19	-28.59	-32.54	-26.22	-30.16	-24.07
CH ₂ γ o	farther ¹ H ^{a)}	-13.36	-23.61	-12.35	-21.56	-11.45	-19.79
	closer ¹ H ^{a)}	-28.61	-23.61	-26.45	-21.73	-24.52	-20.01
CH ₃ o	1st ¹ H	-13.48	-17.30	-12.47	-15.91	-11.56	-14.68
	2nd ¹ H	-15.18	-17.30	-14.04	-15.91	-13.01	-14.68
	3rd ¹ H	-21.58	-17.30	-19.96	-15.91	-18.50	-14.68
	average	-16.75	-17.30	-15.49	-15.91	-14.36	-14.68
CH _{ar} o	XRD ^{c)}	-92.18	-81.04	-85.24	-74.94	-79.02	-69.35

Table S21. Calculated pc s from model (δ_{pc} calc.) vs. experimental hyperfine contributions to the overall observed chemical shifts (δ_{pc} exptl.) in ¹H NMR spectra of **1** dissolved in CD₂Cl₂, at temperatures 265.0 K – 285.0 K. a) Within each methylene group of the outer phthalocyaninato ligands, a distinction is made between the ¹H nuclei based on their distance to the two metal centers of the complex **1**. b) The values of the experimental pseudocontact shift mentioned here correspond to the difference between the observed chemical shifts and the orbital contributions to the chemical shifts. c) The pseudocontact shift for the CH_{ar}o group was calculated as the average value of the pseudocontact shifts of the eight individual CH_{ar}o carbon atoms (see asymmetric unit of **1**, Figure S31).

Group:	Comments:	T [K]					
		295.0		305.0		315.0	
		δ_{pc} calc. [ppm]	δ_{hf} exptl. ^{b)} [ppm]	δ_{pc} calc. [ppm]	δ_{hf} exptl. ^{b)} [ppm]	δ_{pc} calc. [ppm]	δ_{hf} exptl. ^{b)} [ppm]
CH ₂ α i		-82.41	-79.23	-76.63	-73.64	-71.49	-68.57
CH ₂ β i		-43.40	-45.19	-40.35	-42.26	-37.64	-39.58
CH ₂ γ i		-40.29	-39.47	-37.46	-36.81	-34.95	-34.37
CH ₃	1st ¹ H	-25.12	-29.37	-23.36	-27.54	-21.79	-25.83
	2nd ¹ H	-23.88	-29.37	-22.21	-27.54	-20.71	-25.83
	3rd ¹ H	-25.17	-29.37	-23.40	-27.54	-21.83	-25.83
	average	-24.72	-29.37	-22.99	-27.54	-21.45	-25.83
CH _{ar} i		-175.95	-174.69	-163.61	-163.03	-152.62	-152.47
CH ₂ α o	farther ¹ H ^{a)}	-15.27	-22.45	-14.20	-21.02	-13.25	-19.72
	closer ¹ H ^{a)}	-44.90	-43.93	-41.75	-40.37	-38.95	-37.23
CH ₂ β o	farther ¹ H ^{a)}	-15.15	-21.36	-14.09	-19.86	-13.14	-18.50
	closer ¹ H ^{a)}	-28.00	-22.16	-26.04	-20.52	-24.29	-19.05
CH ₂ γ o	farther ¹ H ^{a)}	-10.63	-18.27	-9.88	-16.95	-9.22	-15.73
	closer ¹ H ^{a)}	-22.77	-18.52	-21.17	-17.21	-19.75	-16.03
CH ₃ o	1st ¹ H	-10.73	-13.62	-9.98	-12.70	-9.31	-11.86
	2nd ¹ H	-12.08	-13.62	-11.23	-12.70	-10.48	-11.86
	3rd ¹ H	-17.18	-13.62	-15.97	-12.70	-14.90	-11.86
	average	-13.33	-13.62	-12.39	-12.70	-11.56	-11.86
CH _{ar} o	XRD ^{c)}	-73.36	-64.40	-68.22	-59.97	-63.64	-55.94

Table S22. Calculated pc s from model (δ_{pc} calc.) vs. experimental hyperfine contributions to the overall observed chemical shifts (δ_{pc} exptl.) in ¹H NMR spectra of **1** dissolved in CD₂Cl₂, at temperatures 295.0 K – 315.0 K. a) Within each methylene group of the outer phthalocyaninato ligands, a distinction is made between the ¹H nuclei based on their distance to the two metal centers of the complex **1**. b) The values of the experimental pseudocontact shift mentioned here correspond to the difference between the observed chemical shifts and the orbital contributions to the chemical shifts. c) The pseudocontact shift for the CH_{ar}o group was calculated as the average value of the pseudocontact shifts of the eight individual CH_{ar}o carbon atoms (see asymmetric unit of **1**, Figure S31).

VI. Measured total couplings (Table S23-S26)

Group:	Comments:	<i>T</i> [K]					
		265.0	275.0	285.0	295.0	305.0	315.0
		¹³ C NMR Data: ¹ <i>T</i> (¹³ C- ¹ H) couplings [Hz]					
CH ₂ α _i		35.0	42.0	55.0	65.0	/	82.0
CH ₂ β _i		/	93.0	94.0	94.0	97.0	104.0
CH ₂ γ _i		/	112.4	112.5	113.4	115.0	116.1
CH ₃ _i		113.3	114.0	115.8	116.5	/	119.0
CH _{ar} _i		266.0	249.0	236.0	223.0	215.0	205.0
CH ₂ α _o	1st ¹ H ^{a)}	0.0	23.0	45.0	58.0	71.0	83.5
	2nd ¹ H ^{a)}	70.5	80.0	89.0	96.0	102.5	107.0
CH ₂ β _o	1st ¹ H ^{a)}	110.0	111.0	113.0	113.0	115.0	116.0
	2nd ¹ H ^{a)}	70.0	79.0	88.0	95.0	98.0	102.0
CH ₂ γ _o	^{b)}	/	118.1	120.2	121.6	122.9	123.6
CH ₃ _o		113.0	115.3	117.5	118.4	119.0	120.0
CH _{ar} _o		/	264.0	253.0	242.0	233.0	225.0

Table S23. Measured total ¹³C-¹H couplings, as observed from ¹³C NMR spectra of **1** recorded at different temperatures. The “/” sign indicates the values of the total coupling that were not extractable, due to overlapping signals that could not have been deconvoluted. a) Since the methylene groups of the outer phthalocyaninato ligands are diastereotopic, the corresponding ¹³C nucleus shows a coupling to each of the ¹H nuclei separately. b) For the CH₂γ_o group, a triplet was observed at all temperatures. CD₂Cl₂ was used as a solvent.

Group:	Comments:	T [K]					
		265.0	275.0	285.0	295.0	305.0	315.0
		¹ H NMR Data: ¹ T (¹ H- ¹ H) couplings					
CH ₂ αi		-259.9	-226.3	-194.2	-163.3	-133.0	-101.2
CH ₂ βi		-61.5	-46.6	-35.0	-21.6	N. A.	N. A.
	farther ¹ H	-168.9	-144.0	-122.7	-105.6	-90.7	-75.2
CH ₂ αo	closer ¹ H	-166.6	-141.6	-121.5	-104.7	-87.0	-75.3
	average ^{a)}	-167.8	-142.8	-122.1	-105.2	-88.9	-75.3
	farther ¹ H	-50.9	-42.0	-34.8	-31.8	-22.5	-13.0
CH ₂ βo	closer ¹ H	-50.8	-42.0	-33.9	-31.7	-21.7	-12.9
	average ^{a)}	-50.9	-42.0	-34.4	-31.8	-22.1	-13.0

Table S24. Measured total ¹H-¹H couplings, as observed from ¹H NMR of **1** spectra recorded at different temperatures. CD₂Cl₂ was used as a solvent. For A₂ systems, ¹T_{HH} = 1.5·D_{HH}. a) For the methylene groups of the outer ring, average values of the measured total couplings are taken in further calculations. “N. A.” denotes that no coupling information was extractable at this temperature due to coalescence.

Group:	T [K]					
	265.0	275.0	285.0	295.0	305.0	315.0
	Errors in ¹ T _{CH} from ¹³ C NMR spectra [Hz]					
CH ₂ αi	5.0	5.0	5.0	5.0	/	5.0
CH ₂ βi	/	0.5	2.0	2.0	1.5	1.0
CH ₂ γi	/	0.5	1.0	0.5	1.5	1.5
CH ₃ i	0.5	0.3	0.2	3.0	/	1.0
CH _{ar} i	6.0	5.0	5.0	5.0	5.0	5.0
CH ₂ αo	2.0	2.0	2.0	2.0	1.5	2.0
CH ₂ βo	1.0	1.0	1.0	1.0	0.5	0.5
CH ₂ γo	/	1.0	1.0	1.0	0.5	0.5
CH ₃ o	1.0	0.5	1.0	1.0	2.0	1.5
CH _{ar} o	/	4.0	4.0	3.0	2.5	2.0

Table S25. Errors in reading the values of the total observed ¹³C-¹H couplings in ¹³C NMR spectra of **1** dissolved in CD₂Cl₂, for all temperatures at which spectra were recorded. These errors were estimated by slightly changing the phase of the spectrum or by modifying the linear back-prediction parameter in TopSpin. The errors of the order parameters originate from the errors in this table.

Group:	T [K]					
	265.0	275.0	285.0	295.0	305.0	315.0
	¹ H NMR Data: ¹ T (¹ H- ¹ H) couplings					
CH ₂ α _i	1.5	1.5	1.5	1.5	2.5	1.5
CH ₂ β _i	2.0	3.0	3.5	5.0	N. A.	N. A.
CH ₂ α _o	2.0	1.0	2.0	2.0	2.5	2.0
CH ₂ β _o	2.0	2.0	2.0	2.0	2.0	5.0

Table S26. Errors in reading the values of the total observed ¹H-¹H couplings in ¹H NMR spectra of **1** dissolved in CD₂Cl₂, for all temperatures at which spectra were recorded. These errors were estimated by slightly changing the phase of the spectrum or by modifying the linear back-prediction parameter in TopSpin. The errors of the order parameters originate from the errors in this table.

VII. Dynamic frequency shifts (Eq. S7-S11, Fig. S24, Table S27-S29)

For calculation of the dynamic frequency shift of complex **1**, the equation reported by Ghose and Prestegardⁱⁱⁱ was adapted for two metal centers present in SMM **1**.

$$\Delta\nu_{DFS} = \frac{1}{8\pi} g_e \mu_e \frac{B_0 S_e (S_e + 1)}{kT} \frac{\varepsilon_{DD} \varepsilon_{CSR}}{2r_{AX}^3} \left(\frac{3 \cos^2 \theta_1 - 1}{r_{e1}^3} + \frac{3 \cos^2 \theta_2 - 1}{r_{e2}^3} \right) \frac{\tau_c^2 \omega}{(1 + \omega^2 \tau_c^2)} \quad (S7)$$

where ε_{DD} and ε_{CSR} are given by equations S8 and S9, respectively.

$$\varepsilon_{DD} = -(24 \pi / 5)^{1/2} (\mu_0 / 4 \pi) \hbar \gamma_A \gamma_X \quad (S8)$$

$$\varepsilon_{CSR} = -(24 \pi / 5)^{1/2} (\mu_0 / 4 \pi) \hbar \gamma_A \gamma_e \quad (S9)$$

g_e is the electron g-factor, μ_e is the electronic Bohr magneton, B_0 is the external magnetic field strength (in units of Tesla), S_e is the electronic spin of the terbium ion ($S_e = 3$), μ_0 is the vacuum permeability, γ_A , γ_X and γ_e are the gyromagnetic ratios of the observed nuclei A, its neighboring nuclei X and the electron, respectively, r_{AX} is the distance between nuclei A and X, θ_1 is the angle between the A-one terbium ion and AX vectors, θ_2 is the angle between the A-other terbium ion and AX vectors, r_{e1} is the distance between nucleus A and the first terbium ion, r_{e2} is the distance between the nucleus A and the second terbium ion, τ_c is the correlation time for overall molecular tumbling and ω is the Larmor frequency of nucleus A.

Group:	Comments:	r_{prox} [Å]	θ_{prox} [°]	r_{dist} [Å]	θ_{dist} [°]
CH ₂ α _i		8.5242	58.65	8.5242	79.63
CH ₂ β _i		10.0068	98.24	10.0068	115.48
CH ₂ γ _i		10.8030	71.31	10.8030	86.87
CH ₃ _i	1st ¹ H	12.2811	96.84	12.2811	110.81
	2nd ¹ H	12.2811	120.32	12.2811	120.01
	3rd ¹ H	12.2811	110.33	12.2811	96.67
CH _{ar} _i		5.7945	103.23	5.7945	103.23
CH ₂ α _o	farther ¹ H ^{a)}	8.6244	77.61	10.2042	96.10
	closer ¹ H ^{a)}	8.6244	69.85	10.2042	57.53
CH ₂ β _o	farther ¹ H ^{a)}	10.1208	109.16	11.5756	120.72
	closer ¹ H ^{a)}	10.1208	101.92	11.5756	85.87
CH ₂ γ _o	farther ¹ H ^{a)}	10.9806	89.01	12.4520	103.88
	closer ¹ H ^{a)}	10.9806	72.34	12.4520	62.91
CH ₃ _o	1st ¹ H	12.4400	109.99	13.7753	118.89
	2nd ¹ H	12.4400	122.40	13.7753	123.36
	3rd ¹ H	12.4400	94.75	13.7753	81.19
CH _{ar} _o		5.7887	104.05	7.6076	98.72

Table S27. Coordinates used in equation S7 for calculating the dynamic frequency shift contribution to the total ¹³C-¹H coupling observed in ¹³C NMR spectra of **1**. The coordinates were extracted from the model used for fitting the pseudocontact shifts of the ¹³C resonances. a) The calculated dynamic frequency shifts are different for the two ¹³C-¹H vectors of the methylene groups in the outer phthalocyaninato ligand, and are hence distinguished by qualitatively describing these vectors as having the ¹H nucleus either further away from or closer to the two terbium centers.

¹³ C NMR frequencies taken for DFS calculations		
T [K]	$\omega/2\pi$ [Mhz]	Taken at position ^{a)} [ppm]
265.0	150.88609988	-110.0
275.0	150.88839758	-95.0
285.0	150.88984282	-85.0
295.0	150.89134501	-75.0
305.0	150.89361877	-60.0
315.0	150.89509433	-50.0

Table S28. Frequencies of ¹³C NMR nuclei that were used in the calculation of the dynamic frequency shift contribution to the observed total ¹³C-¹H couplings. a) For all ¹³C NMR resonances of **1** in a spectrum recorded at a given temperature, the middle between the resonances that were most upfield and most downfield was taken as the value of ω in equation S7. This Table refers to spectra recorded with CD₂Cl₂ as solvent.

		T [K]					
		265.0	275.0	285.0	295.0	305.0	315.0
		η [mPa·s]					
		0.588	0.517	0.462	0.419	0.386	0.360
		τ_c [ps]					
		1705	1447	1247	1093	974	879
Group:	Comments:	$\Delta\nu_{DFS}$ in ^{13}C NMR [Hz]					
$\text{CH}_2\alpha\text{i}$		-6.27	-5.46	-4.70	-4.03	-3.47	-2.99
$\text{CH}_2\beta\text{i}$		-4.91	-4.28	-3.68	-3.16	-2.72	-2.34
$\text{CH}_2\gamma\text{i}$		-4.75	-4.14	-3.56	-3.06	-2.63	-2.27
CH_3i	averaged for all three ^1H	-2.35	-2.04	-1.76	-1.51	-1.30	-1.12
$\text{CH}_{\text{ar}}\text{i}$		-31.88	-27.74	-23.90	-20.51	-17.63	-15.20
$\text{CH}_2\alpha\text{o}$	farther $^1\text{H}^{\text{a}}$	-8.02	-6.98	-6.01	-5.16	-4.43	-3.82
	closer $^1\text{H}^{\text{a}}$	-4.03	-3.50	-3.02	-2.59	-2.23	-1.92
$\text{CH}_2\beta\text{o}$	farther $^1\text{H}^{\text{a}}$	-2.82	-2.46	-2.12	-1.82	-1.56	-1.35
	closer $^1\text{H}^{\text{a}}$	-5.25	-4.57	-3.94	-3.38	-2.91	-2.51
$\text{CH}_2\gamma\text{o}$	farther $^1\text{H}^{\text{a}}$	-4.21	-3.67	-3.16	-2.71	-2.33	-2.01
	closer $^1\text{H}^{\text{a}}$	-2.64	-2.30	-1.98	-1.70	-1.46	-1.26
CH_3o	averaged for all three ^1H	-1.69	-1.47	-1.27	-1.09	-0.93	-0.81
$\text{CH}_{\text{ar}}\text{o}$		-23.40	-20.36	-17.54	-15.05	-12.94	-11.16

Table S29. Viscosity data (η) needed for the calculation of the correlation time for overall molecular tumbling (τ_c), τ_c and dynamic frequency shifts calculated from coordinates in Table S27. a) The calculated dynamic frequency shifts are different for the two ^{13}C - ^1H vectors of the methylene groups of the outer phthalocyaninato ligand, and are hence distinguished by qualitatively describing these vectors as having their ^1H nucleus either further away from or closer to the two terbium centers in **1**.

The correlation time for overall molecular tumbling, τ_c , was approximated from Stokes's law, using eq. S10^{iv}:

$$\tau_c = \frac{4\pi r^3 \eta}{3kT} \quad (\text{S10})$$

where τ_c is in seconds, r is the radius of the molecular sphere in meters, η is the viscosity of the solvent in Pa·s, k is the Boltzmann constant and T is the temperature in K. The radius r was approximated by using the largest r_{prox} distance from Table S20 (and corresponding θ_{prox} , belonging to CH_3o), and by using the XRD Tb-Tb distance of complex **1**. The value of r used in eq. S10 was thus 13.635 Å. The values of η for the temperature range from 265.0 K to 315.0 K were taken from the available literature on $\text{CH}_2\text{Cl}_2^{\text{v}}$, as η of CD_2Cl_2 and η of CH_2Cl_2 are nearly identical^{vi} and as viscosity data was available for CD_2Cl_2 only at room temperature.

The calculated values of τ_c ranged from 1705 ps (265.0 K) to 879 ps (315.0 K) and are given in Table S29, as well as the values of η used in equation S10.

The dependence of $\Delta\nu_{DFS}$ on τ_c is shown in the following example, for a ^1H (A) nucleus in a complex with only one metal ion in it. Accordingly, equation S7 becomes equation S11:

$$\Delta\delta_{DFS} = \frac{1}{8\pi} g_e \mu_e \frac{B_0 S_e (S_e + 1)}{kT} \frac{\varepsilon_{DD} \varepsilon_{CSR}}{2r_{AX}^3} \left(\frac{3\cos^2\theta - 1}{r_e^3} \right) \frac{\tau_c^2 \omega}{(1 + \omega^2 \tau_c^2)} \quad (\text{S11}^{\text{vi}})$$

In the example, the B_0 was set to 14.09 T (ω was accordingly set to $2\pi \cdot 600.13$ MHz). It was taken that there is only one metal ion with S_e equal to $3/2$. The neighboring nucleus X was taken to be a ^{13}C one, T was taken to be 298 K, r_{AX} was set to 1.1 Å, r_e was set to 10 Å and θ was set to 0° . The dependence of $\Delta\nu_{DFS}$ on τ_c for this example is presented in Figure S24. This example was reproduced from the work of Ghose and Prestegard.ⁱⁱⁱ

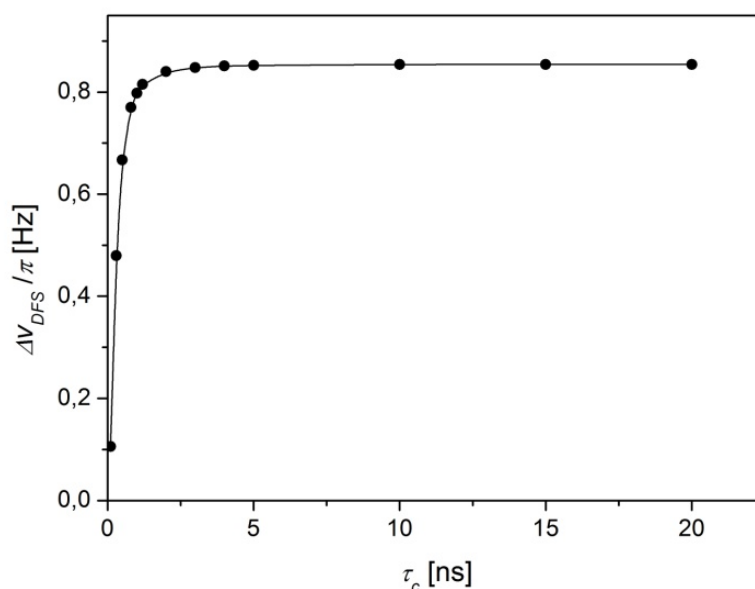


Figure S24. Plot of the variation in the magnitude of the shift of the resonance position of the ^1H component of a ^1H - ^{13}C doublet with a change in the correlation time τ_c , for an exemplary complex with one metal center, where $B_0 = 14.09$ T, $S_e = 3/2$, $T = 295$ K, $r_{ax} = 1.1$ Å, $r_e = 10$ Å and $\theta = 0^\circ$.

VIII. Residual dipolar couplings and the order parameter (Fig. S25-S26, Table S30-S36)

Group:	Comments:	T [K]					
		265.0	275.0	285.0	295.0	305.0	315.0
		D_{CH} from ^{13}C NMR [Hz]					
CH ₂ αi		-99.7	-93.5	-81.3	-72.0	N. A.	-56.0
CH ₂ βi		N. A.	-27.7	-27.3	-27.8	-25.3	-18.7
CH ₂ γi		N. A.	-8.5	-8.9	-8.5	-7.4	-6.6
CH ₃ i		-9.4	-9.0	-7.4	-7.0	N. A.	-4.9
CH _{ar} i		139.5	118.3	101.5	85.1	74.2	61.8
	farther ^1H ^{a)}	-133.0	-111.0	-90.0	-77.8	-65.6	-53.7
CH ₂ αo	closer ^1H ^{a)}	-66.5	-57.5	-49.0	-42.4	-36.3	-32.1
	farther ^1H ^{a)}	-12.2	-11.5	-9.9	-10.2	-8.4	-7.7
CH ₂ βo	closer ^1H ^{a)}	-49.7	-41.4	-33.1	-26.6	-24.1	-20.5
CH ₂ γo	^{b)}	N. A.	-3.9	-2.2	-1.2	-0.2	0.2
CH ₃ o		-10.3	-8.2	-6.2	-5.5	-5.1	-4.2
CH _{ar} o		N. A.	126.0	112.1	98.7	87.5	77.8

Table S30. ^{13}C - ^1H RDCs obtained from ^{13}C NMR spectra of **1** dissolved in CD_2Cl_2 , recorded at different temperatures, at a field strength of 14.09 T. These values were obtained after the subtraction of scalar couplings and calculated DFS contributions from the observed total couplings. “N. A.” denotes cases where the extraction of $^1T_{CH}$ was not possible due to signal broadness or overlaps a) Since the methylene groups of the outer phthalocyaninato ligands are diastereotopic, the corresponding ^{13}C nucleus shows a coupling to each of the ^1H nuclei. b) This ^{13}C NMR resonance gave a triplet, hence only one RDC value was extractable.

Group:	T [K]					
	265.0	275.0	285.0	295.0	305.0	315.0
	D_{HH} [Hz]					
CH ₂ α ⁱ ^{a)}	-173.3	-150.9	-129.5	-108.9	-88.7	-67.5
CH ₂ β ⁱ ^{a)}	-41.0	-31.1	-23.3	-14.4	N. A.	N. A.
CH ₂ α ^o ^{b), c)}	-157.0	-132.0	-110.3	-94.4	-78.1	-64.5
CH ₂ β ^o ^{b), d)}	-38.5	-29.6	-22.0	-19.4	-9.7	-0.6

Table S31. ¹H-¹H RDCs obtained from ¹H NMR spectra of **1** dissolved in CD₂Cl₂, recorded at different temperatures, at a field strength of 14.09 T. a) For A₂ systems, ¹T_{HH} = 1.5·D_{HH}. b) These values correspond to the difference between the averaged ¹T_{HH} (Table S24) and the geminal ¹H-¹H couplings. c) ²J_{H-C-H} = -10.8 Hz (value reported for methanol)^{vii a, d, e, f}. d) ²J_{H-C-H} = -12.4 Hz (value reported for methane).^{vii a, b, c}

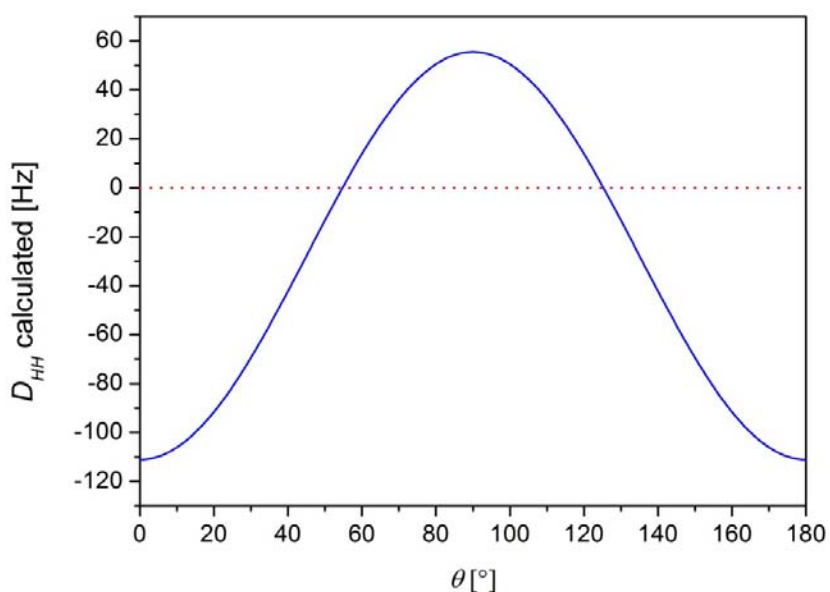


Figure S25. The dependence of the calculated ¹H-¹H RDC from the θ angle in equation 10. For this calculation, T was set to 295.0 K, the ¹H-¹H distance was set to 1.78486 Å and the magnetic susceptibility anisotropy value was taken from Table S7.

Group:	Comments:	T [K]					
		265.0	275.0	285.0	295.0	305.0	315.0
		D_{CH} in ^{13}C NMR spectra as calculated from the model [Hz]					
CH ₂ αi		-134.8	-114.3	-98.0	-82.3	-71.8	-59.8
CH ₂ βi		-135.0	-114.5	-98.2	-82.3	-71.8	-59.8
CH ₂ γi		-135.0	-114.5	-98.2	-82.3	-71.8	-59.8
	1st ¹ H	-140.4	-119.0	-102.1	-85.6	-74.7	-62.2
	2nd ¹ H	134.8	114.3	98.0	82.3	71.8	59.8
CH ₃ i	3rd ¹ H	-129.4	-109.8	-94.1	-79.0	-68.8	-57.3
	averaged ^{b)}	-44.9	-38.2	-32.7	-27.5	-23.9	-20.0
CH _{ar} i		139.4	118.4	101.5	85.2	74.2	61.8
	farther ¹ H ^{a)}	-147.2	-124.9	-107.1	-89.8	-78.4	-65.2
CH ₂ αo	closer ¹ H ^{a)}	-70.7	-60.0	-51.4	-43.2	-37.7	-31.3
	farther ¹ H ^{a)}	-85.8	-72.8	-62.4	-52.4	-45.7	-38.0
CH ₂ βo	closer ¹ H ^{a)}	-143.5	-121.9	-104.5	-87.6	-76.4	-63.6
	farther ¹ H ^{a)}	-195.6	-166.0	-142.3	-119.3	-104.1	-86.6
CH ₂ γo	closer ¹ H ^{a)}	-44.3	-37.5	-32.1	-27.0	-23.5	-19.6
	averaged ^{c)}	-119.9	-101.6	-87.2	-73.1	-63.8	-53.1
	1st ¹ H	-54.1	-45.9	-39.4	-33.0	-28.9	-24.0
	2nd ¹ H	107.9	91.5	78.5	65.8	57.4	47.8
CH ₃ o	3rd ¹ H	-187.6	-159.2	-136.5	-114.6	-99.9	-83.1
	averaged ^{b)}	-44.6	-37.9	-32.4	-27.2	-23.8	-19.7
CH _{ar} o	averaged ^{d)}	136.4	115.8	99.3	83.3	72.6	60.5

Table S32. Static residual ^{13}C - ^1H dipolar couplings as calculated from the modeled structure of **1**. a) The calculated RDCs for the two ^{13}C - ^1H vectors in each methylene group of the outer ligand are different from each other, and are hence distinguished by qualitatively describing how far their ^1H in vectors are from the two terbium centers. b) For the methyl groups of both the inner and outer ligand, the average value of the RDC for the three ^{13}C - ^1H vectors was taken for further calculations. c) For the CH₂γo group, since the ^{13}C resonance gave a triplet, i.e. there is only one observable $^1T_{CH}$, the average of the two values of the calculated RDCs was taken for further calculations. d) For the CH_{ar}o group, the value of the calculated RDC reported in this table represents an average of the RDCs calculated from all eight individual ^{13}C - ^1H vectors in the asymmetric unit of the X-Ray structure, with the C-H bond length set to 1.081 Å. The values reported here were calculated with magnetic susceptibility anisotropy values from Table S36.

Group:	T [K]					
	265.0	275.0	285.0	295.0	305.0	315.0
	D_{HH} in ^1H NMR spectra as calculated from the model [Hz]					
$\text{CH}_2\alpha\text{i}$	-246.3	-209.0	-179.2	-150.3	-131.1	-109.1
$\text{CH}_2\beta\text{i}$	-246.3	-209.0	-179.2	-150.3	-131.1	-109.1
$\text{CH}_2\alpha\text{o}$	-208.7	-177.1	-151.9	-127.4	-111.1	-92.4
$\text{CH}_2\beta\text{o}$	-217.6	-184.5	-158.2	-132.9	-115.8	-96.4

Table S33. Residual ^1H - ^1H dipolar couplings as calculated from the modeled structure of **1**. The values reported here were calculated with magnetic susceptibility anisotropy values from Table S36.

Group:	Comments:	T [K]					
		265.0	275.0	285.0	295.0	305.0	315.0
		Order parameter S , as calculated from D_{CH}					
$\text{CH}_2\alpha\text{i}$		0.74 (0.04)	0.82 (0.04)	0.83 (0.05)	0.87 (0.06)	N. A.	0.94 (0.08)
$\text{CH}_2\beta\text{i}$		N. A.	0.24 (0.01)	0.28 (0.02)	0.34 (0.02)	0.35 (0.03)	0.31 (0.02)
$\text{CH}_2\gamma\text{i}$		N. A.	0.07 (0.01)	0.09 (0.01)	0.10 (0.01)	0.10 (0.02)	0.11 (0.03)
CH_3i		0.21 (0.01)	0.23 (0.01)	0.23 (0.01)	0.25 (0.11)	N. A.	0.24 (0.05)
$\text{CH}_{\text{ar}}\text{i}$		1.00 (0.04)	1.00 (0.04)	1.00 (0.05)	1.00 (0.06)	1.00 (0.09)	1.00 (0.08)
	farther $^1\text{H}^{\text{a}}$	0.90 (0.01)	0.89 (0.02)	0.84 (0.02)	0.87 (0.02)	0.84 (0.06)	0.82 (0.03)
$\text{CH}_2\alpha\text{o}$	closer $^1\text{H}^{\text{a}}$	0.94 (0.03)	0.96 (0.03)	0.95 (0.04)	0.98 (0.05)	0.96 (0.08)	1.02 (0.06)
	average $^{\text{b}}$	0.92 (0.02)	0.92 (0.02)	0.90 (0.03)	0.92 (0.03)	0.90 (0.07)	0.92 (0.05)
	farther $^1\text{H}^{\text{a}}$	0.14 (0.01)	0.16 (0.01)	0.16 (0.02)	0.19 (0.02)	0.18 (0.02)	0.20 (0.01)
$\text{CH}_2\beta\text{o}$	closer $^1\text{H}^{\text{a}}$	0.35 (0.01)	0.34 (0.01)	0.32 (0.01)	0.30 (0.01)	0.32 (0.02)	0.32 (0.01)
	average $^{\text{b}}$	0.24 (0.01)	0.25 (0.01)	0.24 (0.01)	0.25 (0.02)	0.25 (0.02)	0.26 (0.01)
$\text{CH}_2\gamma\text{o}$		N. A.	0.06 (0.02)	0.04 (0.02)	0.03 (0.02)	0.01 (0.01)	0.00 (0.02)
CH_3o		0.23 (0.02)	0.22 (0.01)	0.19 (0.03)	0.20 (0.04)	0.21 (0.08)	0.21 (0.08)
$\text{CH}_{\text{ar}}\text{o}$		N. A.	1.09 (0.03)	1.13 (0.04)	1.18 (0.04)	1.21 (0.09)	1.29 (0.03)

Table S34. Order parameters derived from combining the model fitted to ^{13}C NMR pseudocontact shifts with the experimentally obtained ^{13}C - ^1H residual dipolar couplings. “N. A.” denotes cases where the extraction of $^1T_{CH}$ was not possible due to signal broadness or overlaps. Order parameters were not calculated from data recorded at 265.0 K, because of many signal overlaps. Standard deviations are given in brackets. a) A distinction is made between the two ^{13}C - ^1H vectors of the two diastereotopic methylene groups. b) For the methylene groups whose ^{13}C NMR resonances are doublets of doublets (two RDCs due to both ^{13}C - ^1H vectors were obtained), the final order parameter is taken to be the average of the order parameters calculated from the two ^{13}C - ^1H RDCs.

Group:	T [K]					
	265.0	275.0	285.0	295.0	305.0	315.0
	Order parameter S , as calculated from D_{HH}					
CH ₂ α i	0.704 (0.006)	0.722 (0.007)	0.723 (0.008)	0.724 (0.010)	0.677 (0.019)	0.619 (0.014)
CH ₂ β i	0.166 (0.008)	0.149 (0.014)	0.13 (0.020)	0.096 (0.033)	N. A.	N. A.
CH ₂ α o	0.752 (0.010)	0.745 (0.006)	0.726 (0.013)	0.741 (0.016)	0.703 (0.023)	0.698 (0.022)
CH ₂ β o	0.177 (0.009)	0.16 (0.011)	0.139 (0.013)	0.146 (0.015)	0.084 (0.017)	0.006 (0.052)

Table S35. Order parameters derived from combining the modeled alkyl chains of the inner and outer phthalocyaninato ring with the experimentally obtained ¹H-¹H residual dipolar couplings. Standard deviations are given in brackets.

T [K]	χ_a [m ³]
265.0	20.24E-31
275.0	17.82E-31
285.0	15.84E-31
295.0	13.75E-31
305.0	12.40E-31
315.0	10.66E-31

Table S36. χ_a values as calculated from the residual dipolar couplings of group CH_{ar}i (given in Table S30), using equation 10. r_{CH} was set to 1.081 Å and θ was set to 90°.

IX. Additional information (Eq. S12-S14, Fig. S27-S29, Table S37)

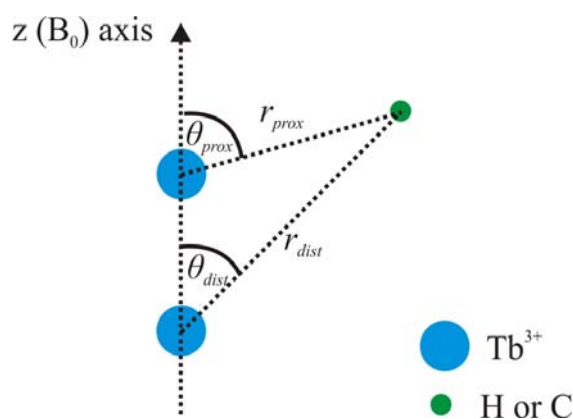


Figure S26. Definitions of θ_{prox} , θ_{dist} , r_{prox} and r_{dist} used in equation 8.

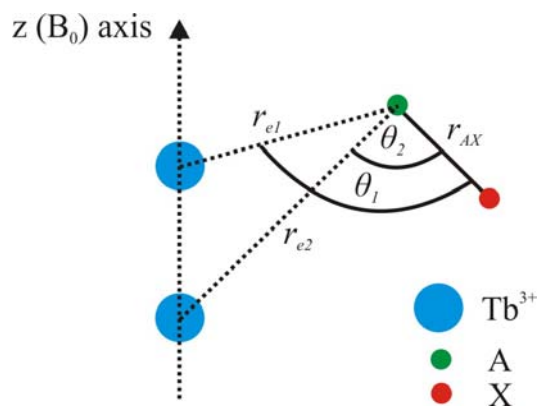


Figure S27. Definitions of θ_1 , θ_2 , r_{e1} , r_{e2} and r_{AX} used in equation S7.

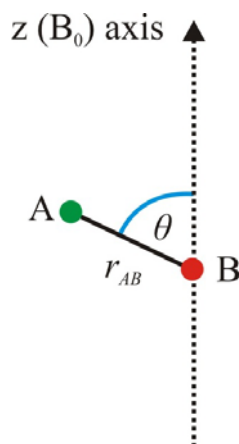


Figure S28. Definitions of θ , and r_{AB} used in equation 10.

Calculating RDCs from the modeled groups

Given here is a description on how the RDCs were calculated from the model. The calculation shown here is for ^{13}C - ^1H RDCs, but the same approach applies to calculating the ^1H - ^1H RDCs.

For every bonded ^{13}C and ^1H nucleus, their coordinates (in terms of distance r and angle θ with their meanings as in Figure S28, relative to any one of the two metal centers of **1**) were taken from the model used to fit the ^{13}C NMR pseudocontact shift data. The distance of the projection of each of these nuclei ($d_{\text{Tb}}^z(^1\text{H})$ and $d_{\text{Tb}}^z(^{13}\text{C})$) on the z axis from the terbium ion was calculated with equations S12-S13:

$$d_{\text{Tb}}^z(^1\text{H}) = r_{\text{H}} \sin(90^\circ - \theta_{\text{H}}) \quad (\text{S12})$$

$$d_{\text{Tb}}^z(^{13}\text{C}) = r_{\text{C}} \sin(90^\circ - \theta_{\text{C}}) \quad (\text{S13})$$

Where r_H and θ_H are the coordinates of the ^1H and r_C and θ_C are the coordinates of the ^{13}C . The difference between $d_{Tb}^z(^1\text{H})$ and $d_{Tb}^z(^{13}\text{C})$ is related to the orientation of the ^{13}C - ^1H vector, as is shown in equation S14:

$$\theta = \arccos\left(\frac{|d_{Tb}^z(^{13}\text{C}) - d_{Tb}^z(^1\text{H})|}{d(\text{C}-\text{H})}\right) \quad (\text{S14})$$

Where θ describes the orientation of the ^{13}C - ^1H vector relative to the B_0 axis (equation 10, Figure S28) and $d(\text{C}-\text{H})$ is the length of the C-H bond (values as reported in the main text). With $d(\text{C}-\text{H})$ and θ known, it was possible to calculate the RDCs given in Table S32 (accordingly, Table S33 for ^1H - ^1H RDCs).

Compound 1

IUPAC Name:

Terbium, [μ -[2,3,9,10,16,17,23,24-octabutoxy-29H,31H-phthalocyaninato(2-)- $\kappa\text{N}^{29},\kappa\text{N}^{30},\kappa\text{N}^{31},\kappa\text{N}^{32}:\kappa\text{N}^{29},\kappa\text{N}^{30},\kappa\text{N}^{31},\kappa\text{N}^{32}$]]bis[2,3,9,10,16,17,23,24-octabutoxy-29H,31H-phthalocyaninato(2-)- $\kappa\text{N}^{29},\kappa\text{N}^{30},\kappa\text{N}^{31},\kappa\text{N}^{32}$]]di-Coordination Compound;

CAS Registry Number:

1269611-92-8;

Chemical Formula:

$\text{C}_{192} \text{H}_{240} \text{N}_{24} \text{O}_{24} \text{Tb}_2$;

Commonly abbreviated in literature as:

$\text{Tb}_2(\text{obPc})_3$.

Constant	Symbol	Value
Gyromagnetic ratio for a ^1H nucleus	γ_H	$2.67522128 \cdot 10^8 \text{ s}^{-1} \text{ T}^{-1}$
Gyromagnetic ratio for a ^{13}C nucleus	γ_C	$6.728284 \cdot 10^7 \text{ s}^{-1} \text{ T}^{-1}$
Gyromagnetic ratio for an isolated electron	γ_e	$-1.760859708 \cdot 10^{11} \text{ s}^{-1} \text{ T}^{-1}$
Boltzmann constant	k	$1.380658 \cdot 10^{-23} \text{ J K}^{-1}$
Vacuum permeability	μ_0	$1.256367061 \cdot 10^{-6} \text{ H m}^{-1}$
Planck constant	h	$6.6260755 \cdot 10^{-34} \text{ J s}$
	\hbar	$1.05457266 \cdot 10^{-34} \text{ J s}$
Electron g-factor	g_e	-2.002319304
Electronic Bohr magneton	μ_e	$9.27400968 \cdot 10^{-24} \text{ J T}^{-1}$

Table S37. Physical constants used in this work.^{viii}

X. Experimental section (Table S38)

Terbium triple decker **1** was prepared according to a published procedure.^{ix}

NMR spectra were recorded at 7.9 T with a Bruker Avance II instrument equipped with a BBFO probe and at 14.09 T with a Bruker Avance III instrument equipped with a QNP Cryoprobe (inner coil tuned to ¹³C, cold preamplifier). Temperatures have been calibrated using the method of Berger et al.^x Solvent resonances were taken as references for all ¹H and ¹³C NMR spectra.

The deuterated solvents (CD₂Cl₂, toluene-d⁸, Sigma-Aldrich) were dried before use.

NMR Experiments

Experiment:	¹ H NMR		¹³ C NMR	¹³ C { ¹ H} NMR
<i>B</i> ₀ [T]:	7.90	14.09	14.09	14.09
Pulse Sequence:	zg30	zg30	zg	zgdc
Sweep Width [ppm]:	500	500	592	592
Acquisition Time [sec]:	0.1089867	0.1089867	0.1822912	0.0917504
Dwell Time [μsec]:	2.500	1.667	5.600	5.600
Pre-Scan Delay [μsec]:	6.500	10.000	100.0	100.0
Frequency of Channel 1 [ppm]:	-100.000	-200.000	-150.000	-150.000
Relaxation Delay [μsec]:	0.200	0.050	0.050	0.050
Channel 1 - 90° Pulse Duration [μsec]:	11.50	14.60	12.00	12.00
Second Channel:	/	/	/	¹ H
CPD program:	/	/	/	garp4
Channel 2 - 90° Pulse Duration [μsec]:	/	/	/	70.00
Frequency of Channel 2 [ppm]:	/	/	/	-6.000

Table S38. Basic parameters used for acquiring 1D NMR spectra on instruments mentioned above.

The ¹³C NMR spectra were processed in the following way: After zero filling to 64k real data points the first points of the FID were eliminated and typically 96 data points were backpredicted in order to reduce base line rolling. An exponential window function (e.g. lb=5Hz) was applied or a lorentz-gauss transformation (lb=-10Hz, gb=0.2).

The referencing was done by using the resonances of the solvent signals. The values were taken from the work of Fulmer et al..^{xi}

¹H NMR of complex 1:

(600.13 MHz, in CD₂Cl₂, *T* = 265.0 K)

δ [ppm] = -210.86 (s, 2H, CH_{ar}i), -95.93 (d, *T*(H,H) = -259.9 Hz, 4H, CH₂ α i), -73.54 (s, 4H, CH_{ar}o), -54.38 (d, *T*(H,H) = -61.5 Hz, 4H, CH₂ β i), -53.68 (d, *T*(H,H) = -166.6 Hz, 4H, CH₂ α o), -47.99 (s, 4H, CH₂ γ i), -35.16 (s, 6H, CH₃i), -26.83 (d, *T*(H,H) = -50.8 Hz, 4H, CH₂ β o), -25.36 (d, *T*(H,H) = -50.9 Hz, 4H, CH₂ β o), -24.05 (d, *T*(H,H) = -168.9 Hz, 4H, CH₂ α o), -22.16 (s, 8H, CH₂ γ o), -16.40 (s, 12H, CH₃o).

(600.13 MHz, in CD₂Cl₂, *T* = 275.0 K)

δ [ppm] = -194.94 (s, 2H, CH_{ar}i), -88.33 (d, *T*(H,H) = -226.3 Hz, 4H, CH₂ α i), -67.44 (s, 4H, CH_{ar}o), -50.40 (d, *T*(H,H) = -46.6 Hz, 4H, CH₂ β i), -48.55 (d, *T*(H,H) = -141.6 Hz, 4H, CH₂ α o), -44.33 (s, 4H, CH₂ γ i), -32.73 (s, 6H, CH₃i), -24.46 (d, *T*(H,H) = -42.0 Hz, 4H, CH₂ β o), -23.25 (d, *T*(H,H) = -42.0 Hz, 4H, CH₂ β o), -21.93 (d, *T*(H,H) = -144.0 Hz, 4H, CH₂ α o), -20.28 (s, 4H, CH₂ γ o), -20.11 (s, 4H, CH₂ γ o), -16.40 (s, 12H, CH₃o).

(600.13 MHz, in CD₂Cl₂, *T* = 285.0 K)

δ [ppm] = -180.25 (s, 2H, CH_{ar}i), -81.39 (d, *T*(H,H) = -194.2 Hz, 4H, CH₂ α i), -61.85 (s, 4H, CH_{ar}o), -46.70 (d, *T*(H,H) = -35.0 Hz, 4H, CH₂ β i), -43.93 (d, *T*(H,H) = -121.5 Hz, 4H, CH₂ α o), -41.00 (s, 4H, CH₂ γ i), -30.49 (s, 6H, CH₃i), -22.31 (d, *T*(H,H) = -33.9 Hz, 4H, CH₂ β o), -21.32 (d, *T*(H,H) = -34.8 Hz, 4H, CH₂ β o), -20.04 (d, *T*(H,H) = -122.7 Hz, 4H, CH₂ α o), -18.56 (s, 4H, CH₂ γ o), -18.34 (s, 4H, CH₂ γ o), -13.78 (s, 12H, CH₃o).

(600.13 MHz, in CD₂Cl₂, *T* = 295.0 K)

δ [ppm] = -167.19 (s, 2H, CH_{ar}i), -75.17 (d, *T*(H,H) = -163.3 Hz, 4H, CH₂ α i), -56.90 (s, 4H, CH_{ar}o), -43.43 (d, *T*(H,H) = -21.6 Hz, 4H, CH₂ β i), -39.87 (d, *T*(H,H) = -104.7 Hz, 4H, CH₂ α o), -38.02 (s, 4H, CH₂ γ i), -28.47 (s, 6H, CH₃i), -20.40 (d, *T*(H,H) = -31.7 Hz, 4H, CH₂ β o), -19.60 (d, *T*(H,H) = -31.8 Hz, 4H, CH₂ β o), -18.39 (d, *T*(H,H) = -105.6 Hz, 4H, CH₂ α o), -17.07 (s, 4H, CH₂ γ o), -16.82 (s, 4H, CH₂ γ o), -12.72 (s, 12H, CH₃o).

(600.13 MHz, in CD₂Cl₂, *T* = 305.0 K)

δ [ppm] = -155.53 (s, 2H, CH_{ar}i), -69.58 (d, *T*(H,H) = -133.0 Hz, 4H, CH₂ α i), -52.47 (s, 4H, CH_{ar}o), -40.50 (s, 4H, CH₂ β i), -36.31 (d, *T*(H,H) = -87.0 Hz, 4H, CH₂ α o), -35.36 (s, 4H, CH₂ γ i), -26.64 (s, 6H, CH₃i), -18.76 (d, *T*(H,H) = -21.7 Hz, 4H, CH₂ β o), -18.10 (d, *T*(H,H) = -22.5 Hz, 4H, CH₂ β o), -16.96 (d, *T*(H,H) = -90.7 Hz, 4H, CH₂ α o), -15.76 (s, 4H, CH₂ γ o), -15.50 (s, 4H, CH₂ γ o), -11.80 (s, 12H, CH₃o).

(600.13 MHz, in CD₂Cl₂, *T* = 315.0 K)

δ [ppm] = -144.95 (s, 2H, CH_{ar}i), -64.51 (d, *T*(H,H) = -101.2 Hz, 4H, CH₂ α i), -48.44 (s, 4H, CH_{ar}o), -37.82 (s, 4H, CH₂ β i), -33.17 (d, *T*(H,H) = -75.3 Hz, 4H, CH₂ α o), -32.92 (s, 4H, CH₂ γ i), -24.93 (s, 6H, CH₃i), -17.29 (d, *T*(H,H) = -12.9 Hz, 4H, CH₂ β o), -16.74 (d, *T*(H,H) = -13.0 Hz, 4H, CH₂ β o), -15.66 (d, *T*(H,H) = -75.2 Hz, 4H, CH₂ α o), -14.58 (s, 4H, CH₂ γ o), -14.28 (s, 4H, CH₂ γ o), -10.96 (s, 12H, CH₃o).

(600.13 MHz, in toluene-d⁸, *T* = 295.0 K)

δ [ppm] = -140.98 (s, 2H, CH_{ar}i), -65.53 (d, *T*(H,H) = -158.0 Hz, 4H, CH₂ α i), -37.73 (s, 4H, CH_{ar}o), -34.94 (broad s, 4H, CH₂ β i), -32.01 (s, 4H, CH₂ γ i), -30.63 (d, *T*(H,H) = -81.6 Hz, 4H, CH₂ α o), -22.72 (s, 6H, CH₃i), -13.51 (s, 8H, CH₂ β o), -8.64 (d, *T*(H,H) = -104.0 Hz, 4H, CH₂ α o), -11.30 (s, 8H, CH₂ γ o), -8.09 (s, 12H, CH₃o).

¹³C NMR of complex 1:

(600.13 MHz, in CD₂Cl₂, *T* = 295.0 K)

δ [ppm] = -252.1 (*v*_{1/2} = 215.7 Hz, s, C_qi), -86.5 (*v*_{1/2} = 175.7 Hz, d, ¹*T*_{CH} = 223.0 Hz, CH_{ar}i), -63.3 (*v*_{1/2} = 179.3 Hz, s, C_qo), -19.6 (*v*_{1/2} = 24.7 Hz, t, ¹*T*_{CH} = 113.4 Hz, CH₂ γ i), -17.4 (*v*_{1/2} = 32.3 Hz, t, ¹*T*_{CH} = 94.0 Hz, CH₂ β i), -16.7 (*v*_{1/2} = 21.2 Hz, q, ¹*T*_{CH} = 116.5 Hz, CH₃i), -4.1 (*v*_{1/2} = 44.5 Hz, t, ¹*T*_{CH} = 65.0 Hz, CH₂ α i), -0.8 (*v*_{1/2} = 56.6 Hz, s, C_qo_i), 0.0 (*v*_{1/2} = 16.4 Hz, q, ¹*T*_{CH} = 118.4 Hz, CH₃o), 1.7 (*v*_{1/2} = 28.1 Hz, t, ¹*T*_{CH} = 121.6 Hz, CH₂ γ o), 9.3 (*v*_{1/2} = 27.8 Hz, dd, ¹*T*_{1stCH} = 95.0 Hz, ¹*T*_{2ndCH} = 113.0 Hz, CH₂ β o), 23.8 (*v*_{1/2} = 126.7 Hz, d, ¹*T*_{CH} = 242.0 Hz, CH_{ar}o), 37.9 (*v*_{1/2} = 47.4 Hz, dd, ¹*T*_{1stCH} = 58.0 Hz, ¹*T*_{2ndCH} = 96.0 Hz, CH₂ α o), 94.8 (*v*_{1/2} = 36.2 Hz, s, C_qo_o).

(600.13 MHz, in toluene-d⁸, *T* = 295.0 K)

δ [ppm] = -210.2 (*v*_{1/2} = 262.4 Hz, s, C_qi), -56.5 (*v*_{1/2} = 139.2 Hz, d, ¹*T*_{CH} = 210.2 Hz, CH_{ar}i), -49.2 (*v*_{1/2} = 223.4 Hz, s, C_qo), -13.4 (*v*_{1/2} = 26.2 Hz, t, ¹*T*_{CH} = 111.1 Hz, CH₂ γ i), -10.8 (*v*_{1/2} = 20.8 Hz, q, ¹*T*_{CH} = 88.0 Hz, CH₃i), -8.6 (*v*_{1/2} = 29.2 Hz, t, ¹*T*_{CH} = 88.0 Hz, CH₂ β i), 4.8 (*v*_{1/2} = 18.1 Hz, q, ¹*T*_{CH} = 119.1 Hz, CH₃o), 6.3 (*v*_{1/2} = 44.3 Hz, t, ¹*T*_{CH} = 56.0 Hz, CH₂ α i), 7.2 (*v*_{1/2} = 30.7 Hz, t, ¹*T*_{CH} = 125.4 Hz, CH₂ γ o), 16.4 (*v*_{1/2} = 29.3 Hz, t, ¹*T*_{CH} = 107.7 Hz, CH₂ β o), 19.4 (*v*_{1/2} = 72.4 Hz, s, C_qo_i), 42.2 (*v*_{1/2} = 116.7 Hz, d, ¹*T*_{CH} = 242.2 Hz, CH_{ar}o), 47.0 (*v*_{1/2} = 20.1 Hz, dd, ¹*T*_{1stCH} = 45.9 Hz, ¹*T*_{2ndCH} = 116.9 Hz, CH₂ α o), 112.0 (*v*_{1/2} = 45.7 Hz, s, C_qo_o).

XI. X-ray structure of complex **1** (Fig. S30-S32)

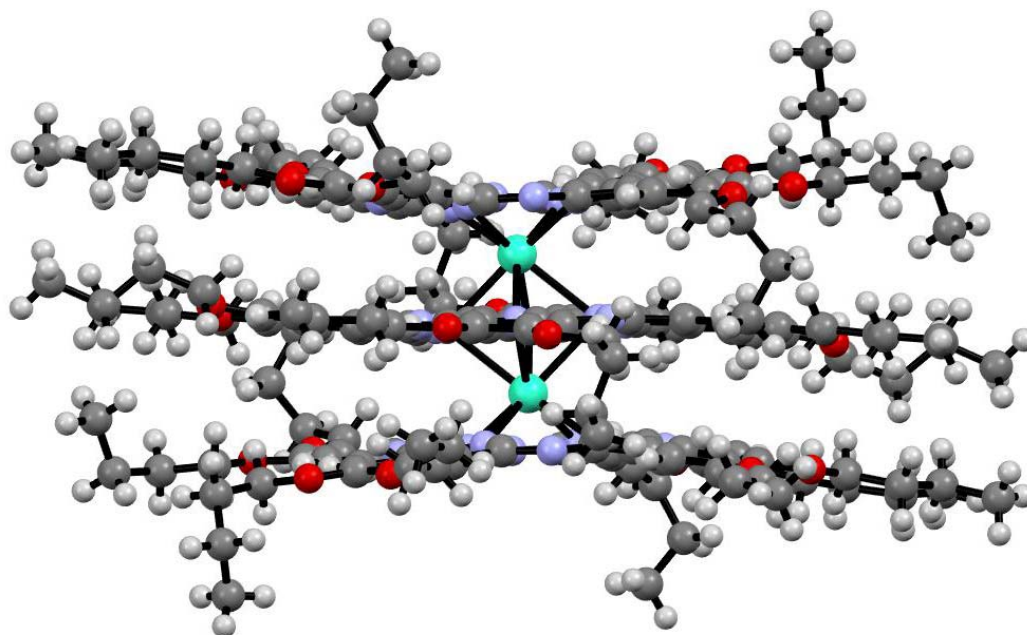


Figure S29. Crystal structure of complex **1**, side view.^{xii}

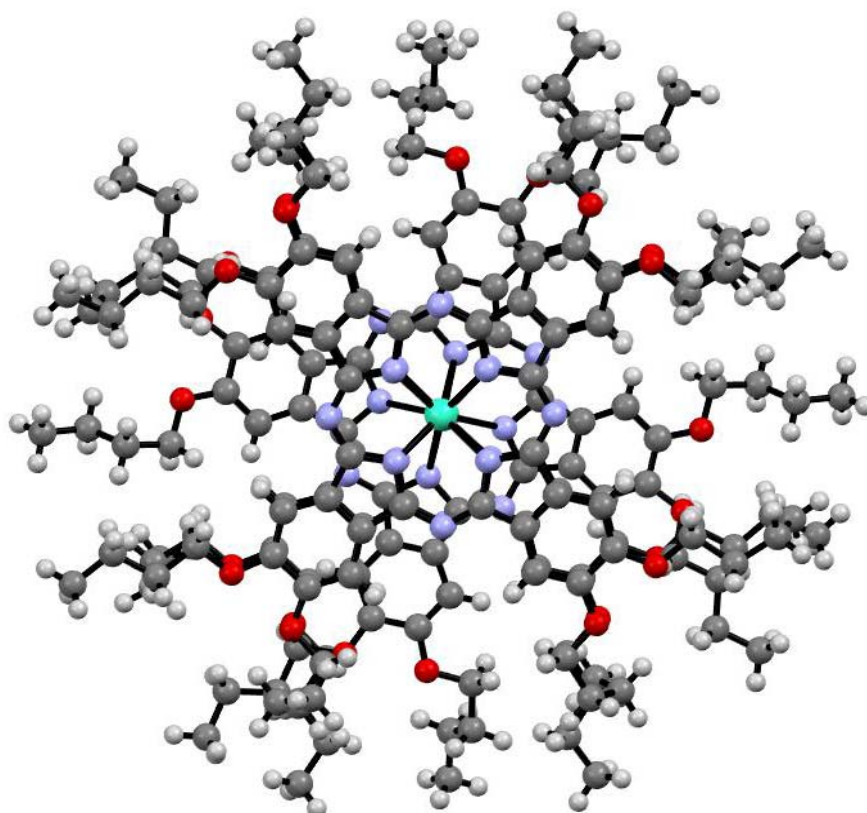


Figure S30. Crystal structure of complex **1**, top view.^{xii}

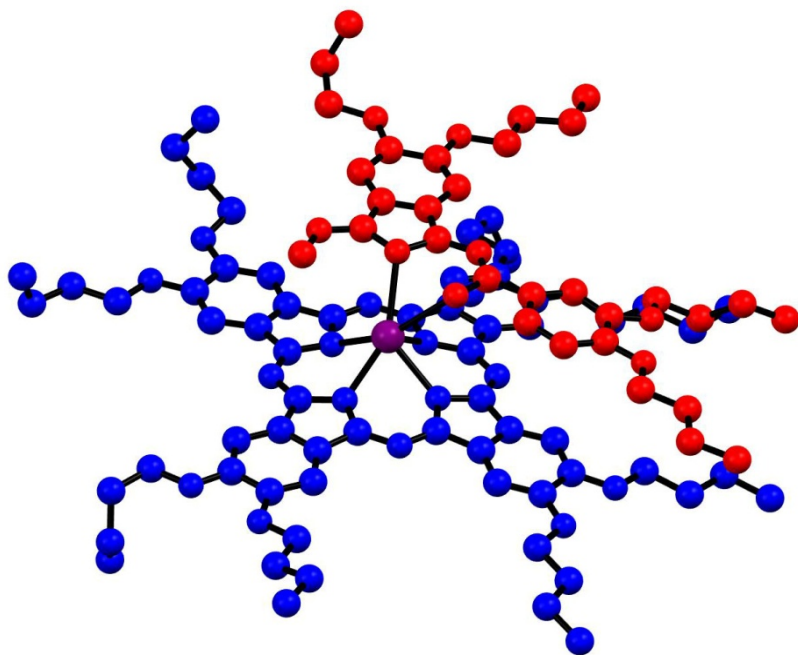


Figure S31. The asymmetric unit of complex **1**. Atoms of the inner ligand are colored red and atoms of the outer ligand are colored blue. The one terbium ion of the asymmetric unit is given here in purple color. Hydrogen atoms have been omitted for clarity.^{xii}

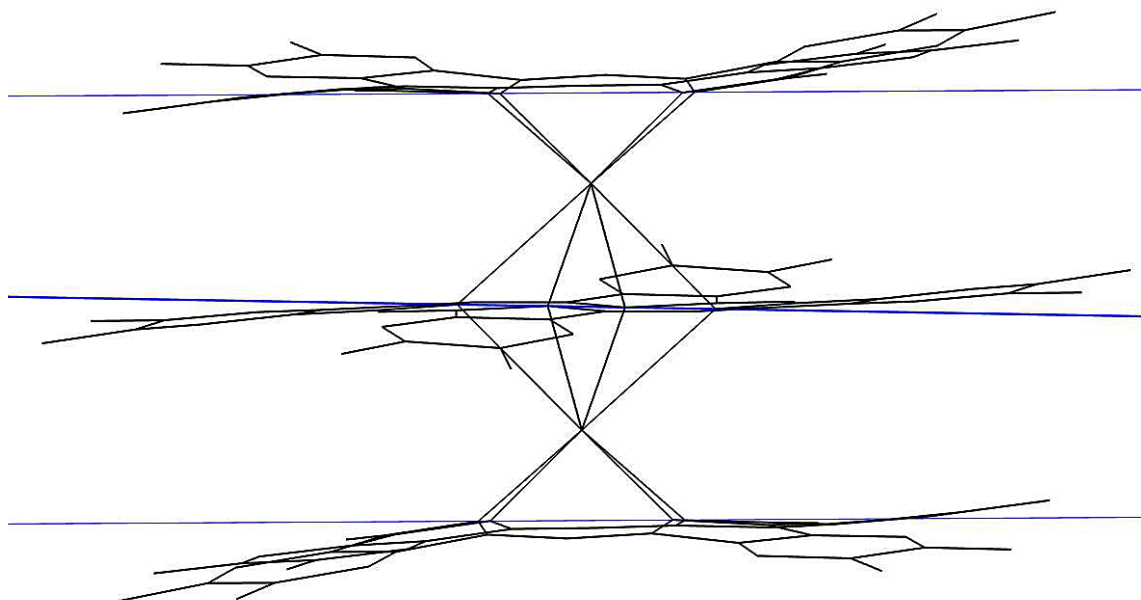


Figure S32. Wireframe side view of the crystal structure of complex **1**. For clarity, butyl groups have been omitted. Blue horizontal lines denote the planes of the phthalocyaninato ligands. In this perspective, distortions of the isoindole moieties from the planes of the rings are clearly visible.^{xii}

XII. Literature

-
- (i) (a) Fürst, A.; Pretsch, E. *Anal. Chim. Acta* **1990**, *229*, 17. (b) Pretsch, E.; Fürst, A.; Badertscher, M.; Bürgin, R.; Munk, M. E. *J. Chem. Inf. Comp. Sci.* **1992**, *32*, 291. (c) Bürgin Schaller, R.; Pretsch, E. *Anal. Chim. Acta* **1994**, *290*, 295. (d) Bürgin Schaller, R.; Arnold, C.; Pretsch, E. *Anal. Chim. Acta* **1995**, *312*, 95. (e) Bürgin Schaller, R.; Munk, M. E.; Pretsch, E. *J. Chem. Inf. Comput. Sci.* **1996**, *36*, 239.
- (ii) Ishikawa, N.; Iino, T.; Kaizu, Y. *J. Phys. Chem. A* **2003**, *107*, 7879.
- (iii) Ghose, R.; Prestegard, J. H. *J. Magn. Reson.* **1997**, *128*, 138.
- (iv) Cavanagh, J.; Fairbrother, W. J.; Palmer, A. G.; Rance, M.; Skelton, N. J. *Protein NMR Spectroscopy: Principles and Practice* (2nd Ed.), Academic Press, New York, London, **2006**.
- (v) (a) Timmermans, J.; Hennaut-Roland, M. *J. Chim. Phys.* **1932**, *29*, 529. (b) Pal, C.; Kumar, A. *Fl. Phase Eq.* **1998**, *143*, 241. (c) Phillips, T. W.; Murphy, K. P. *J. Chem. Eng. Data* **1970**, *15*, 304.
- (vi) Li, D.; Kagan, G.; Hopson, R.; Williard, P. G. *J. Am. Chem. Soc.* **2009**, *131*, 5627.
- (vii) (a) Pople, J. A.; Bothner-By, A. A. *J. Chem. Phys.* **1965**, *42*, 1339. (b) Bernstein, H. J.; Sheppard, N. *J. Chem. Phys.* **1962**, *37*, 3012. (c) Anet, F. A. L. *J. Am. Chem. Soc.* **1962**, *84*, 3767. (d) Barfield, M.; Grant, D. M. *J. Am. Chem. Soc.* **1961**, *83*, 4726. (e) Barfield, M.; Grant, D. M. *J. Chem. Phys.* **1962**, *36*, 2054. (f) Barfield, M.; Grant, D. M. *J. Am. Chem. Soc.* **1963**, *85*, 1899.
- (viii) Atkins, P.; de Paula, J. *Atkin's Physical Chemistry, 9th ed.*, Oxford University Press, **2009**.
- (ix) Takahashi, K.; Itoh, M.; Tomita, Y.; Nojima, K.; Kasuga, K.; Isa, K. *Chem. Lett.* **1993**, 1915.
- (x) Findeisen, M.; Brand, T.; Berger, S. *Magn. Reson. Chem.* **2007**, *45*, 175.
- (xi) Fulmer, G. R.; Miller, A. J. M.; Sherden, N. H.; Gottlieb, H. E.; Nudelman, A.; Stoltz, B. M.; Bercaw, J. E.; Goldberg, K. I. *Organometallics* **2010**, *29*, 2176.
- (xii) Katoh, K.; Horii, Y.; Yasuda, N.; Wernsdorfer, W.; Toriumi, K.; Breedlove, B. K.; Yamashita, M. *Dalton Trans.* **2012**, *41*, 13582.